

Computational Science Laboratory  
Report CSL-TR-21-10  
November 30, 2021

Amit N Subrahmanya, Andrey A Popov,  
Adrian Sandu

*“An Ensemble Variational Fokker-Planck  
Method for Data Assimilation”*

Computational Science Laboratory  
“Compute the Future!”

Department of Computer Science  
Virginia Tech  
Blacksburg, VA 24060  
Phone: (540) 231-2193  
Fax: (540) 231-6075

Email: [amitns@vt.edu](mailto:amitns@vt.edu), [apopov@vt.edu](mailto:apopov@vt.edu), [sandu@cs.vt.edu](mailto:sandu@cs.vt.edu)  
Web: <https://csl.cs.vt.edu>



# AN ENSEMBLE VARIATIONAL FOKKER-PLANCK METHOD FOR DATA ASSIMILATION \*

AMIT N SUBRAHMANYA <sup>†</sup>, ANDREY A POPOV<sup>†</sup>, AND ADRIAN SANDU<sup>†</sup>

**Abstract.** Particle flow filters that aim to smoothly transform particles from samples from a prior distribution to samples from a posterior are a major topic of active research. In this work we introduce a generalized framework which we call the Variational Fokker-Planck method for filtering and smoothing in data assimilation that encompasses previous methods such as the mapping particle filter and the particle flow filter. By making use of the properties of the optimal Itô process that solves the underlying Fokker-Planck equation we can explicitly include heuristics methods such as rejuvenation and regularization that fit into this framework. We also extend our framework to higher dimensions using localization and covariance shrinkage, and provide a robust implicit-explicit method for solving the stochastic initial value problem describing the Itô process. The effectiveness of the variational Fokker-Planck method is demonstrated on three test problems, namely the Lorenz '63, Lorenz '96 and the quasi-geostrophic equations.

**Key words.** Data Assimilation, Bayesian Inference, Particle Filter

**AMS subject classifications.** 65C05, 93E11, 62F15, 86A22

**1. Introduction.** Data assimilation (DA) [4, 31] aims to estimate the states of a physical system by optimally combining sparse and noisy observations of the truth with forecasts obtained via model evolution through inference techniques. As exact Bayesian inference is computationally intractable, statistical sampling methods are frequently used to perform approximate inference, which can introduce the curse of dimensionality [15].

Popular statistical methods for assimilation include the Ensemble Kalman Filter (EnKF) [5, 10, 11] and the Ensemble Kalman Smoother (EnKS) [12] and related methods. Ensemble collapse—also called filter divergence—occurs when the covariance of the ensemble forecast becomes extremely small, that the filter discards the observations, making the analysis trajectory diverge from the truth. Popular heuristics to prevent collapse include anomaly inflation [27], and particle rejuvenation [7, 28] In high-dimensional problems, estimates of statistics such as the covariance are inaccurate, requiring heuristic fixes such as localization [3] and covariance shrinkage [6].

An alternative to Kalman-filter based methods are particle filters [40] that make little to no assumptions about any of the involved distributions. These methods suffer from degeneracy over time requiring resampling of the particles. Most particle filters are infeasible as they require an exorbitantly large number of particles to successfully assimilate observations. More robust approaches to particle filter such as the Ensemble Transport Particle Filter (ETPF) [1] and the Marginal Adjusted Rank Histogram Filter (MARHF) [2] are being developed, but these methods require further research to be operationally viable.

In this work we focus on an intermediate step from fully Gaussian methods such as the EnKF to parameterized variants of non-Gaussian methods based on particle flow [23] through the Fokker-Planck equations [18, 32]. The mapping particle filter (MPF) [29] was the first major foray into this family of methods. It aims to make

---

\*Submitted to the arXiv November 30, 2021.

**Funding:** This work was supported by DOE through grant ASCR DE-SC0021313, and by the Computational Science Laboratory at Virginia Tech.

<sup>†</sup>Computational Science Laboratory, Department of Computer Science, Virginia Tech, Blacksburg, VA (amitns@vt.edu, apopov@vt.edu, sandu@cs.vt.edu).

use of a reproducing kernel Hilbert space to compute the flow that minimizes the KL-divergence [21] between distributions fully defined by the particles involved. The particle flow filter (PFF) introduced in [16], performs a localized semi-Gaussian flow in order to extend the methodology to higher-dimensional problems. In this work we introduce the Variational Fokker-Planck approach to data assimilation. Our methodology provides for a way to use arbitrarily parameterized combination of distributions to perform inference. We show how our methodology can be trivially extended to smoothing and localization. We also show that previous methods such as the MPF and the PFF are merely variants in our classification.

While previous work [16,29] has viewed the particle flow problem through the lens of optimization, more recent work [32,34] has viewed the underlying Itô process that evolves each particle from a sample of one distribution to the sample from another as a stochastic initial value problem. A major challenge with this view is dealing with the stiff dynamics of the Itô process. We aim to resolve this problem by introducing a new time-stepping scheme for solving medium-scale stochastic initial value problems suitable for particle-flow applications.

The key contributions of this paper are (i) a generalized formulation of the variational Fokker-Planck approach aimed towards data assimilation, (ii) derivation of the drift of an Itô process to minimize the Kullback-Leibler divergence between the forecast and posterior distributions, (iii) derivation of regularization to ensure particle diversity by minimizing the mutual information between particles, and (iv) derivation of partitioned implicit-explicit (IMEX) time stepping method to evolve the said Itô process.

The remainder of this paper is organized as follows. The general discrete time data assimilation problem is formalized and discussed in section 2 along with a description of notation. In section 3, we (i) derive the KL-divergence minimizing drift, (ii) discuss the application of the derived drift towards ensemble variation data assimilation, (iii) derive a regularizing drift that minimizes the mutual information between particles, (iv) derive an IMEX time-stepping scheme whose strong order is 0.5 to apply to the Itô process, (v) discuss various flavors of our generalized Fokker-Planck approach for filtering and smoothing along with two examples, and (vi) discuss localization and covariance shrinkage to correct estimated covariance in high dimensional problems. Next, we describe experiments on Lorenz '63 [25,37], Lorenz '96 [24,39] and quasi-geostrophic equations [35] in section 4 followed by concluding remarks in section 5.

**2. Background.** Let  $\mathbf{x}_{t,k} \in \mathbb{R}^n$  represent the true state of a dynamical system at time  $t_k$ . Our prior uncertainty is described by the distribution of the random variable  $X_{f,k} \sim \pi_{f,k}$ , called the forecast. Let  $Y_k \sim \pi_{o,k}$  denote a noisy and sparse observation of the truth,

$$(2.1) \quad Y_k = \mathcal{H}_k(\mathbf{x}_{t,k}) + \boldsymbol{\epsilon}_k^o, \quad Y_k \in \mathbb{R}^{n_y}$$

where  $\mathcal{H}_k : \mathbb{R}^n \rightarrow \mathbb{R}^{n_y}$  is a non-linear observation operator, and  $\boldsymbol{\epsilon}_k^o$  is observation error. It is assumed that the observation error distribution  $\pi_{o,k}$  is known. In most operational problems of interest, the observations are spatially sparse i.e  $n_y \ll n$ .

Our goal is to perform Bayesian inference on these two sources of information to obtain a better understanding of the truth,

$$(2.2) \quad \pi_{a,k}(\mathbf{x}) = \pi_{f,k}(\mathbf{x}|\mathbf{y}) \propto \pi_{o,k}(\mathbf{y}|\mathbf{x})\pi_{f,k}(\mathbf{x}),$$

which we denote by  $X_{a,k} \sim \pi_{a,k}$ , for the analysis. The posterior distribution  $\pi_{a,k}$

represents the sum total of our knowledge about the state at time  $t_k$ .

By propagating the analysis forward in time,

$$(2.3) \quad X_{f,k+1} = \mathcal{M}_k(X_{a,k}) + \epsilon_k^f,$$

through the model operator  $\mathcal{M}_k : \mathbb{R}^n \rightarrow \mathbb{R}^n$ , a new prior is obtained at time  $t_{k+1}$ , and the cycle can begin anew. The model forecast error term  $\epsilon_k^f$  we take to be zero for the remainder of this paper.

In the filtering approach to the Bayesian inference problem (2.2) we incorporate only the observation at the current time. If instead we incorporate multiple present and future observations into our current analysis,

$$(2.4) \quad \pi_{a,k}(X_{a,k}) = \pi_{f,k}(X_{f,k} | \mathbf{y}_{k,\dots,k+K}) = \left[ \prod_{i=0}^K \frac{\pi_{o,k+i}(Y_{k+i} | X_{f,k})}{\pi_{o,k+i}(Y_{k+i})} \right] \pi_{f,k}(X_{f,k}),$$

we get the smoothing approach to data assimilation.

In practice, performing exact Bayesian inference is infeasible. This issue can be side-stepped through the use of Monte-Carlo sampling methods. An ensemble of  $N$  realizations of some random variable  $\mathbf{x}$ ,

$$(2.5) \quad \mathbf{X} \in \mathbb{R}^{n \times N} \text{ where } \mathbf{X} = [\mathbf{x}^{[1]} \quad \mathbf{x}^{[2]} \quad \dots \quad \mathbf{x}^{[N]}].$$

denotes an approximation to our knowledge about said random variable. In the ensemble limit of  $N \rightarrow \infty$ , the empirical measure distribution of the ensemble,

$$(2.6) \quad \tilde{\pi}(\mathbf{x}) = \frac{1}{N} \sum_{i=1}^N \delta_{\mathbf{x}^{[i]}}(\mathbf{x}),$$

converges almost surely to the distribution of the random variable  $\pi(\mathbf{x})$ . When the ensemble denotes the state of some dynamical system, each ensemble member is called a particle to denote its propagation through some dynamics. We use this convention for the remainder of this paper.

Particles can be used to estimate statistics such as mean, and covariance, that are defined as

$$(2.7) \quad \bar{\mathbf{x}} = \frac{1}{N} \mathbf{X} \mathbf{1}_N, \quad \mathbf{P} = \mathbf{A} \mathbf{A}^T, \quad \text{with } \mathbf{A} = \frac{1}{\sqrt{N-1}} (\mathbf{X} - \bar{\mathbf{x}} \mathbf{1}_N^T),$$

where  $\mathbf{1}_p$  is used to represent a  $p$ -dimensional vector of ones and  $\mathbf{I}_p$  is used to represent an  $p$ -dimensional identity matrix.

**3. Variational Fokker-Planck for Data Assimilation.** Following the Stein Variational approach to particle flow [23] and the Mapping Particle Filter [29], we generalize these methods into the Variational Fokker-Planck (VFP) approach to data assimilation.

The Fokker-Planck equation describes the evolution of a probability distribution under some external force [21]. A flow is defined if the external force minimizes the KL-divergence [22] between the prior distribution  $\pi_f$  and the posterior distribution  $\pi_a$ . Take a realization from the prior distribution, which we call a particle. The flow of this particle along the distributions defined by the Fokker-Planck equation is driven by an Itô process. This flow completely describes the continuous transformation of

the particle from a realization of the prior random variable, to a realization of the posterior random variable.

The prior and posterior distributions are taken to be parametric. Assuming that it is possible to estimate the parameters of the distributions through ensemble statistics, the flow of each particle in the ensemble can be described only by the information contained in the prior ensemble and the observation. This idea makes up the core of the VFP.

**3.1. Derivation of the VFP method..** A general Itô process that acts on a random variable  $X_s \in \mathbb{R}^n$  is,

$$(3.1) \quad dX_s = \mathbf{v}(X_s)ds + \boldsymbol{\sigma}(X_s)d\mathbf{W}_s, \quad X_{s=0} = X_f,$$

where  $\mathbf{v}(X_s) \in \mathbb{R}^n$  is the drift,  $\boldsymbol{\sigma}(X_s) \in \mathbb{R}^{n \times \ell}$  is the diffusion coefficient,  $d\mathbf{W}_s \in \mathbb{R}^\ell$  is the  $\ell$ -dimensional standard Wiener process and  $s$  is the pseudo-time of the flow.

The Fokker-Planck equation representing the the evolution of the density of  $X_s$  in (3.1) is given by,

$$(3.2) \quad \begin{aligned} \frac{\partial \pi_s(\mathbf{x})}{\partial s} &= - \sum_{i=1}^n \frac{\partial}{\partial \mathbf{x}_i} (\pi_s(\mathbf{x}) \mathbf{v}_i(X_s)) + \sum_{i=1}^n \sum_{j=1}^n \frac{\partial^2}{\partial \mathbf{x}_i \partial \mathbf{x}_j} (\pi_s(\mathbf{x}) \mathbf{D}_{i,j}(X_s)), \\ &= - \nabla_{\mathbf{x}}^T \left( (\pi_s(\mathbf{x}) \cdot \mathbf{v}(X_s)) - (\nabla_{\mathbf{x}}^T (\pi_s(\mathbf{x}) \cdot \mathbf{D}(X_s)))^T \right), \end{aligned}$$

where  $\pi_s(\mathbf{x})$  is the probability density of  $X_s$  and  $\mathbf{D}_{i,j}(X_s) = \boldsymbol{\sigma}(X_s) \boldsymbol{\sigma}^T(X_s)$ . We call the indexed family  $\{\mathbf{X}_s\}_{0 \leq s < \infty}$ , the family of intermediate random variables distributed by the family of intermediate distributions  $\{\pi_s\}_{0 \leq s < \infty}$ .

Following [23], given an initial random variable  $X_f$  with distribution  $\pi_f$ , we wish to find the drift term  $\mathbf{v}(X_s)$ , that causes the family of intermediate random variables to converge in KL-divergence to the random variable  $X_a \sim \pi_a$ ,

$$(3.3) \quad \lim_{s \rightarrow \infty} D_{\text{KL}}(\pi_s \parallel \pi_a) = 0,$$

which we denote by  $X_s \xrightarrow{D} X_a$ .

We now provide the optimal drift term that accomplishes this goal.

**THEOREM 3.1.** *The drift  $\mathbf{v}(X_s)$  of the Itô process (3.1) that minimizes the KL-divergence (3.3) of the family of distributions governed by the Fokker-Planck equation (3.2) is given by,*

$$(3.4) \quad \mathbf{v}(X_s) = \nabla_{\mathbf{x}} \log \pi_a(\mathbf{x}) + (\mathbf{D}(X_s) - \mathbf{I}_n) \nabla_{\mathbf{x}} \log \pi_s(\mathbf{x}) + (\nabla_{\mathbf{x}}^T \mathbf{D}(X_s))^T,$$

under the assumption that  $\forall s$ ,  $\text{support}(\pi_s) \subseteq \text{support}(\pi) := \Omega$ .

*Proof.* Omitting all explicit arguments to the probability distributions and functions, the KL-divergence between  $\pi_s$  and  $\pi_a$  is given by,

$$D_{\text{KL}}(\pi_s \parallel \pi_a) = \int_{\Omega} \pi_s \log \left( \frac{\pi_s}{\pi_a} \right) d\mathbf{x}.$$

where  $\Omega$  denotes  $\text{support}(\pi_a)$ . Taking the derivative of the KL-divergence (3.3),

$$\frac{dD_{\text{KL}}}{ds} = \int_{\Omega} \frac{\partial \pi_s}{\partial s} \left( \log \left( \frac{\pi_s}{\pi_a} \right) + 1 \right) d\mathbf{x},$$

which by applying the Fokker-Planck equation (3.2) becomes,

$$\frac{dD_{\text{KL}}}{ds} = \int_{\Omega} -\nabla_{\mathbf{x}}^{\text{T}} \left[ (\pi_s \mathbf{v}) - (\nabla_{\mathbf{x}}^{\text{T}} (\pi_s \mathbf{D}))^{\text{T}} \right] \left[ \log \left( \frac{\pi_s}{\pi_a} \right) + 1 \right] d\mathbf{x}.$$

Assuming  $\pi_s|_{\partial\Omega} \rightarrow 0$ , and integrating by parts,

$$\frac{dD_{\text{KL}}}{ds} = \int_{\Omega} \left( \pi_s \mathbf{v} - (\nabla_{\mathbf{x}}^{\text{T}} (\pi_s \mathbf{D}))^{\text{T}} \right)^{\text{T}} \nabla_{\mathbf{x}} \left( \log \left( \frac{\pi_s}{\pi_a} \right) \right) d\mathbf{x},$$

which we can rewrite as,

$$\frac{dD_{\text{KL}}}{ds} = \int_{\Omega} \left( \pi_s (\mathbf{v} - \mathbf{D}(\nabla_{\mathbf{x}} \log \pi_s) - (\nabla_{\mathbf{x}}^{\text{T}} \mathbf{D})^{\text{T}}) \right)^{\text{T}} \nabla_{\mathbf{x}} \log \left( \frac{\pi_s}{\pi_a} \right) d\mathbf{x}.$$

Minimizing the inner product inside the integral minimizes the gradient. Ignoring  $\pi_s$  as a scaling coefficient, and re-introducing the arguments to all functions, the drift,

$$\mathbf{v}(X_s) = \nabla_{\mathbf{x}} \log \pi_a(\mathbf{x}) + (\mathbf{D}(X_s) - \mathbf{I}_n) \nabla_{\mathbf{x}} \log \pi_s(\mathbf{x}) + (\nabla_{\mathbf{x}}^{\text{T}} \mathbf{D}(X_s))^{\text{T}}$$

for the Itô process (3.1) minimizes the KL-divergence (3.3) in the limit of  $s \rightarrow \infty$ , as required.  $\square$

REMARK 1. *Since  $\mathbf{v}(\mathbf{x}, s)$  can be scaled by any other positive function of  $\mathbf{x}$ , other natural choices include,*

$$(3.5) \quad \mathbf{v}(X_s) = \pi_s(\mathbf{x}) \left( \nabla_{\mathbf{x}} \log \pi_a(\mathbf{x}) + (\mathbf{D}(X_s) - \mathbf{I}_n) \nabla_{\mathbf{x}} \log \pi_s(\mathbf{x}) + (\nabla_{\mathbf{x}}^{\text{T}} \mathbf{D}(X_s))^{\text{T}} \right),$$

$$(3.6) \quad \mathbf{v}(X_s) = \mathbf{F}_{X_s}(\mathbf{x}) \left( \nabla_{\mathbf{x}} \log \pi_a(\mathbf{x}) + (\mathbf{D}(X_s) - \mathbf{I}_n) \nabla_{\mathbf{x}} \log \pi_s(\mathbf{x}) + (\nabla_{\mathbf{x}}^{\text{T}} \mathbf{D}(X_s))^{\text{T}} \right),$$

where  $\mathbf{F}_{X_s}(\mathbf{x}) \in \mathbb{R}^{n \times n}$  is a suitable symmetric positive definite matrix.

There are two terms of interest in the optimal drift (3.4). The term,

$$(3.7) \quad \nabla_{\mathbf{x}} \log \pi_a(\mathbf{x}) - \nabla_{\mathbf{x}} \log \pi_s(\mathbf{x}),$$

is the difference in the gradients log-likelihoods of the analysis and the intermediate distribution. This ensures that point-wise, the features of the distribution, such as the dominant modes, mean, covariance, and higher-order moments, are all approximated equally well. The term,

$$(3.8) \quad \mathbf{D}(X_s) \nabla_{\mathbf{x}} \log \pi_s(\mathbf{x}) + (\nabla_{\mathbf{x}}^{\text{T}} \mathbf{D}(X_s))^{\text{T}},$$

is a dampening of the stochastic term of the Itô process (3.1),

$$(3.9) \quad \sigma(X_s) d\mathbf{W}_s,$$

ensuring that the perturbations to any one realization of intermediate variable still move it towards being a realization of the analysis.

**3.2. Discretization and parameterization of the VFP.** Assume now that we have an ensemble  $\mathbf{X}_s \in \mathbb{R}^{n \times N}$  of  $N$  realizations of the random variable  $X_s$ . We now present a discretization of the method proposed in subsection 3.1 to perform particle flow on a finite ensemble. Define the Itô process acting on the ensemble at pseudo time  $s$  as,

$$(3.10) \quad d\mathbf{X}_s = \mathbf{v}(\mathbf{X}_s) ds + \sigma(\mathbf{X}_s) d\mathbf{W}_s, \quad \mathbf{X}_0 = \mathbf{X}_f,$$

Mixture	$\pi(\mathbf{x}; \Theta_{1\dots m}(\mathbf{x})) \propto \sum_i^m w_i \pi_i(\mathbf{x}; \Theta_i(\mathbf{x}))$ $\nabla_{\mathbf{x}} \log \pi(\mathbf{x}; \Theta_{1\dots m}(\mathbf{x})) = \frac{\sum_i^m w_i (\frac{\partial}{\partial \mathbf{x}} \pi_i(\mathbf{x}; \Theta_i(\mathbf{x})) + \frac{\partial \Theta_i}{\partial \mathbf{x}} \pi_i(\mathbf{x}; \Theta_i(\mathbf{x})) \frac{\partial \Theta_i}{\partial \mathbf{x}})}{\sum_i^m w_i \pi_i(\mathbf{x}; \Theta_i(\mathbf{x}))}$ <p>Simplifying assumption: For all <math>i</math>, <math>\frac{\partial \Theta_i}{\partial \mathbf{x}} = 0</math></p>
Kernel(K)	$\pi(\mathbf{x}) \propto \frac{1}{N} \sum_i^N \mathcal{K}(\mathbf{x} - \mathbf{x}_i)$ $\nabla_{\mathbf{x}} \log \pi(\mathbf{x}) = \frac{\sum_i^N \nabla_{\mathbf{x}} \mathcal{K}(\mathbf{x} - \mathbf{x}_i)}{\sum_i^N \mathcal{K}(\mathbf{x} - \mathbf{x}_i)}$ <p><math>\mathcal{K}</math> is a positive definite kernel</p>
Gaussian(G)	$\pi(\mathbf{x}) \propto \exp(-\frac{1}{2}(\mathbf{x} - \bar{\mathbf{x}})^T \mathbf{P}^{-1}(\mathbf{x} - \bar{\mathbf{x}}))$ $\nabla_{\mathbf{x}} \log \pi(\mathbf{x}) = -\mathbf{P}^{-1}(\mathbf{x} - \bar{\mathbf{x}})$
Laplace(L)	$\pi(\mathbf{x}) \propto (\theta^\nu) \mathcal{K}_\nu(\theta)$ $\nabla_{\mathbf{x}} \log \pi(\mathbf{x}) = -\frac{2}{\theta} \frac{\mathcal{K}_{\nu-1}(\theta)}{\mathcal{K}_\nu(\theta)} \mathbf{P}^{-1}(\mathbf{x} - \bar{\mathbf{x}})$ $\theta = \sqrt{2(\mathbf{x} - \bar{\mathbf{x}})^T \mathbf{P}^{-1}(\mathbf{x} - \bar{\mathbf{x}})}, \quad \nu = \frac{2-n}{2}$ <p><math>\mathcal{K}_\nu</math> is the modified Bessel function of the second kind</p>
Huber(H)	<p>We make a Huber assumption on the Laplace distribution</p> $\nabla_{\mathbf{x}} \log \pi(\mathbf{x}) = \begin{cases} -\delta_1 \frac{2}{\theta} \frac{\mathcal{K}_\nu(\theta)}{\mathcal{K}_\nu(\theta)} \mathbf{P}^{-1}(\mathbf{x} - \bar{\mathbf{x}}) & \delta_1 \frac{2}{\theta} \frac{\mathcal{K}_\nu(\theta)}{\mathcal{K}_\nu(\theta)} < \delta_2, \\ -\delta_2 \mathbf{P}^{-1}(\mathbf{x} - \bar{\mathbf{x}}) & \text{otherwise.} \end{cases}$
Cauchy(C)	$\pi(\mathbf{x}) \propto \frac{1}{(1+(\mathbf{x}-\bar{\mathbf{x}})^T \mathbf{P}^{-1}(\mathbf{x}-\bar{\mathbf{x}}))^{\frac{n+1}{2}}}$ $\nabla_{\mathbf{x}} \log \pi(\mathbf{x}) = -\frac{n+1}{1+(\mathbf{x}-\bar{\mathbf{x}})^T \mathbf{P}^{-1}(\mathbf{x}-\bar{\mathbf{x}})} \mathbf{P}^{-1}(\mathbf{x} - \bar{\mathbf{x}})$

Table 3.1: A collection of several distributions and their gradient-logs. The letters in the parentheses represent abbreviations of the distributions that we use to name the various families of VFP methods. For most of the distributions listed, the parameterizations depend on a semblance of centering  $\bar{\mathbf{x}}$ , which can, but does not necessarily stand for the mean, and a semblance of spread  $\mathbf{P}$ , which can but does not necessarily stand for covariance.

with the initial condition given by the forecast ensemble  $\mathbf{X}_f$ ,  $\mathbf{v} : \mathbb{R}^{n \times N} \rightarrow \mathbb{R}^{n \times N}$  is the deterministic drift,  $\boldsymbol{\sigma} : \mathbb{R}^{n \times N} \rightarrow \mathbb{R}^{n \times \ell}$  is the diffusion coefficient, and  $\mathbf{W}_s \in \mathbb{R}^{\ell \times N}$  is an ensemble of  $\ell$ -dimensional Wiener processes.

Take the drift term  $\mathbf{v}$  to be the optimal drift defined in [Theorem 3.1](#). As the drift acts on realizations of  $\mathbf{X}_s$ , the optimal drift acting on the ensemble transforms each particle into a realization from the posterior distribution  $\pi_a$  given by [\(2.2\)](#) or [\(2.4\)](#). The drift term [Theorem 3.1](#) acting on the ensemble  $\mathbf{X}_s$  can be written as,

$$(3.11) \quad \mathbf{v}(\mathbf{X}_s) = \nabla_{\mathbf{x}} \log \pi_a(\mathbf{X}_s) + (\mathbf{D}(\mathbf{X}_s) - \mathbf{I}_n) \nabla_{\mathbf{x}} \log \pi_s(\mathbf{X}_s) + (\nabla_{\mathbf{x}}^T \mathbf{D}(\mathbf{X}_s))^T,$$

where the analysis and intermediate distributions ( $\pi_a$  and  $\pi_s$  respectively) will be

parameterized by the intermediate ensemble  $\mathbf{X}_s$ .

Since the chosen drift is proven to minimize the KL-divergence between the intermediate family of random variables and the analysis, in the limit of time, each ensemble member in  $\mathbf{X}_s$  converges to a realization of the analysis  $X_a$ . In such a scenario we assume that in the limit of pseudo-time,  $\mathbf{X}_s$  is a suitable analysis ensemble,

$$(3.12) \quad \mathbf{X}_a := \lim_{s \rightarrow \infty} \mathbf{X}_s,$$

where the time evolution of the Itô process (3.10) is performed via a suitable time-stepping scheme.

REMARK 2. *In practice, we can terminate the integration in (3.12) at some finite time  $s^*$  when the change in the statistical mean of  $\mathbf{X}_s$  given by  $\bar{\mathbf{x}}_s$  is under a chosen tolerance threshold,*

$$(3.13) \quad s^* = s + h, \text{ such that } \left\| \left( \frac{\bar{\mathbf{x}}_{s+h} - \bar{\mathbf{x}}_s}{h} \right) \right\| < \epsilon,$$

where  $h$  is the step-size of the time-stepping method and  $\epsilon$  is the tolerance threshold.

The drift term (3.11) requires explicit gradient-log-likelihoods of two distributions: the intermediate  $\pi_s(\mathbf{x})$  and the posterior  $\pi_a(\mathbf{x})$ . In this work, we focus on parameterized families of distributions where the parameters can be estimated from the ensembles. Table 3.1 provides a non-exhaustive list of parameterized families of distributions. Of note are the multivariate Gaussian distribution representing assumptions similar to ensemble Kalman filter methods, the multivariate Laplace and Huber distributions representing methods from robust statistics [30], and the reproducing Kernel Hilbert space assumption from [29]. The terms  $\bar{\mathbf{x}}$  and  $\mathbf{P}$  represent statistical assumptions on the mean and covariance respectively.

REMARK 3. *In the Huber distribution assumption,  $\delta_1$  and  $\delta_2$  are designed such that increasing  $\delta_1$  makes the distribution more Laplace and increasing  $\delta_2$  makes the distribution more Gaussian.*

REMARK 4. *A general approach to a mixture distribution involving an arbitrary set of parameters is also provided in Table 3.1, but is not further analyzed in this work.*

By Bayes' rule (2.2) the analysis gradient-log-likelihood can be parameterized by the sum of two gradient-log-likelihoods,

$$(3.14) \quad \nabla_{\mathbf{x}} \log \pi_a = \nabla_{\mathbf{x}} \log \pi_f + \nabla_{\mathbf{x}} \log \pi_o,$$

where the first term is the gradient-log-likelihood of the prior distribution and the second on the observation distribution. Although the analysis is parameterized in terms of the prior distribution, the assumption on the intermediate distribution  $\pi_s$  does not have to match that of the prior. Therefore in the discretized and parameterized method, there are three steps to parameterizing the method:

1. assume the prior distribution  $\pi_f$ ,
2. calculate the posterior  $\pi_a \propto \pi_f \pi_o$ ,
3. assume the intermediate family  $\pi_s$ .

The choices on the prior and intermediate distributions dictate the parameterization of the method. We use the abbreviations in Table 3.1 to distinguish between them. For instance, we use the notation VFP(GH) to indicate a Gaussian assumption on the prior distribution and a Huber assumption on the intermediate family.

While (3.14) is valid for the filtering setting, in the smoothing (2.4) setting,

$$(3.15) \quad \nabla_{\mathbf{x}} \log \pi_a = \nabla_{\mathbf{x}} \log \pi_f + \sum_{k=1}^K \nabla_{\mathbf{x}} \log \pi_{o,k},$$

is a more explicit formulation of the gradient log-likelihood.

REMARK 5. *The Mapping Particle Filter [29] can be thought of as a Kernel assumption on the prior distribution and a Kernel assumption on the intermediate family, therefore, we consider the the MPPF to be similar to VFP(KK).*

REMARK 6. *It is possible that the choices of parameterized families lead us to intermediate distributions that do not converge in KL-divergence to the analysis (3.3). In that case we look at a weaker criteria for convergence, first order optimality,*

$$(3.16) \quad \lim_{s \rightarrow \infty} \nabla_{\mathbf{x}} D_{\text{KL}}(\pi_s(\mathbf{x}), \pi_a(\mathbf{x})) = 0$$

where the intermediate family of distributions converges to a local minimum of the implicit optimization procedure. As the optimal drift term always points in the direction of minimizing the KL-divergence by Theorem 3.1, this is always true.

To fully discretize the method, we finally have to choose the diffusion term  $\sigma(\mathbf{X}_s)$  in (3.11). When choosing the diffusion, care must be taken to ensure that the stochastic dynamics are faithful to the physics of the actual system. Some good choices for  $\sigma(X_s)$  are the scaled forecast anomalies  $\tau \mathbf{A}_f$ , and the scaled square-root of a climatological covariance  $\tau \mathbf{B}^{\frac{1}{2}}$ . In these cases, since  $\sigma$  is constant,  $(\nabla_{\mathbf{x}}^T \mathbf{D}(X_s))^T = 0$ . The scaling parameter  $\tau$  is of great heuristic interest. There is a strong connection between diffusion and rejuvenation in particle filters [1, 28].

**3.3. Regularization.** While diffusion in the Itô process (3.10) ensures that each ensemble member is a realization from the analysis distribution, there is no guarantee that information described by the ensemble is maximized. Therefore, we propose a type of regularization that would increase the total information content described by the ensemble. From an information theoretic perspective, ensuring particle diversity would require minimizing the mutual information between particles. We now derive a regularizing drift for a cost function that combines the KL-divergence of the intermediate with a target with the mutual information of the intermediate random variable.

THEOREM 3.2. *The regularizing drift  $\mathbf{v}_{\text{MI}}$  that minimizes the mutual information between two random variables  $X$  and  $\hat{X}$  defined on the same probability space  $(\Omega, \mathcal{F}, \pi_s)$  is given by*

$$(3.17) \quad \mathbf{v}_{\text{MI}}(X) = -\alpha \int_{\Omega} \pi_s(\hat{\mathbf{x}}) \kappa(X, \hat{\mathbf{x}}) d\hat{\mathbf{x}},$$

with  $\alpha > 0$ , assuming the coupled joint distribution is,

$$(3.18) \quad \pi_s(\mathbf{x}, \hat{\mathbf{x}}) = R(\mathbf{x}, \hat{\mathbf{x}}) \pi_s(\mathbf{x}) \pi_s(\hat{\mathbf{x}}).$$

where  $R$  is a smooth and positive definite coupling function chosen such that  $\int \pi(\mathbf{x}, \hat{\mathbf{x}})$  integrates to 1, and  $\kappa = R \log(R)$ .

*Proof.* The mutual information between  $X$  and  $\hat{X}$  is given by

$$I(X; \hat{X}) = \int_{\Omega} \pi_s(\hat{\mathbf{x}}) \left( \int_{\Omega} \pi_s(\mathbf{x}|\hat{\mathbf{x}}) \log \left( \frac{\pi_s(\mathbf{x}|\hat{\mathbf{x}})}{\pi_s(\mathbf{x})} \right) d\mathbf{x} \right) d\hat{\mathbf{x}},$$

where  $\mathbf{x}$  and  $\hat{\mathbf{x}}$  are realizations of  $X$  and  $\hat{X}$  respectively. Using the coupling between  $X$  and  $\hat{X}$ , we can rewrite the mutual information as

$$I(X; \hat{X}) = \int_{\Omega} \pi_s(\hat{\mathbf{x}}) \left( \int_{\Omega} \pi_s(\mathbf{x}) R(\mathbf{x}, \hat{\mathbf{x}}) \log R(\mathbf{x}, \hat{\mathbf{x}}) d\mathbf{x} \right) d\hat{\mathbf{x}}.$$

Rewriting  $\kappa = R \log(R)$  and switching the order of integration, we have

$$I(X; \hat{X}) = \int_{\Omega} \pi_s(\mathbf{x}) \left( \int_{\Omega} \pi_s(\hat{\mathbf{x}}) \kappa(\mathbf{x}, \hat{\mathbf{x}}) d\hat{\mathbf{x}} \right) d\mathbf{x}.$$

Scaling the mutual information with  $\alpha$  and adding it to the KL-divergence, we get

$$\widehat{D}_{\text{KL}}(\pi_s(\mathbf{x}) \parallel \pi_a(\mathbf{x})) = D_{\text{KL}}(\pi_s(\mathbf{x}) \parallel \pi_a(\mathbf{x})) + \alpha I(X; \hat{X}),$$

which, when expanded can be written as,

$$\widehat{D}_{\text{KL}} = \int_{\Omega} \pi_s(\mathbf{x}) \left( \log \left( \frac{\pi_s(\mathbf{x})}{\pi_a(\mathbf{x})} \right) + \alpha \int_{\Omega} \pi_s(\hat{\mathbf{x}}) \kappa(\mathbf{x}, \hat{\mathbf{x}}) d\hat{\mathbf{x}} \right) d\mathbf{x}.$$

Following the steps outlined in [Theorem 3.1](#), the modified drift  $\hat{\mathbf{v}}(\mathbf{x})$ , can be written as,

$$\hat{\mathbf{v}}(X) = \mathbf{v}(X) - \alpha \int_{\Omega} \pi_s(\hat{\mathbf{x}}) \kappa(X, \hat{\mathbf{x}}) d\hat{\mathbf{x}},$$

as required.  $\square$

Discretizing the regularized drift given by [Theorem 3.2](#), for each individual intermediate particle  $\mathbf{x}_s^{[j]}$ ,

$$(3.19) \quad \hat{\mathbf{v}}(\mathbf{x}_s^{[j]}) = \mathbf{v}(\mathbf{x}_s^{[j]}) - \frac{\alpha}{N} \sum_{i=1}^N \nabla_{\mathbf{x}} \kappa(\mathbf{x}_s^{[j]}, \mathbf{x}_s^{[i]}),$$

we get an analytical expression in terms of the optimal drift from [Theorem 3.1](#). Here  $\kappa$  is empirically chosen based on the requirements of the specific problem.

One interesting choice for  $\kappa$  is,

$$(3.20) \quad \kappa = \frac{1}{(\|\mathbf{x} - \hat{\mathbf{x}}\|_2)}, \text{ we have } \nabla_{\mathbf{x}} \kappa = -\frac{\mathbf{x} - \hat{\mathbf{x}}}{\|\mathbf{x} - \hat{\mathbf{x}}\|_2^3},$$

which looks exactly like the electrostatic repulsive force according to Coulomb's Law. We utilize [\(3.20\)](#) for the remainder of the paper.

**3.4. Time stepping.** In [\[32\]](#), it is concluded that the Fokker-Planck approach requires further research in time stepping schemes as the pseudo-time evolution is stiff and requires infeasibly small time steps when used with an explicit time-stepping method. For this purpose, we propose an implicit-explicit (IMEX) partitioning of the dynamics. In an IMEX method, stiff (or fast) dynamics are solved implicitly and the

non-stiff (or slow) dynamics are solved explicitly. Take the Itô process (3.1), flow from time  $s_i$  to time  $s_{i+1}$ ,

$$(3.21) \quad \mathbf{z}_{s_{i+1}} = \mathbf{z}_{s_i} + \int_{s_i}^{s_{i+1}} \mathbf{v}(\mathbf{z}_s) ds + \int_{s_i}^{s_{i+1}} \boldsymbol{\sigma}(\mathbf{z}_s) d\mathbf{W}_s,$$

of some variable of interest  $\mathbf{z}$ . We can partition the system into fast dynamics,  $\mathbf{v}^{\{\text{f}\}}(\mathbf{z}_s)$  representing the drift term, and the slow dynamics  $\boldsymbol{\sigma}^{\{\text{s}\}}(\mathbf{z}_s)$  representing diffusion.

As implicit methods are computationally expensive, we instead choose to look at linearly implicit methods whose the computational cost is moderate but provide stable solutions for relatively larger time-steps. We propose to solve the fast dynamics of the drift with the linearly implicit Rosenbrock-Euler scheme [36] and the slow dynamics of the diffusion with the Euler-Maruyama scheme. Discretizing (3.21) with the proposed scheme, one step of the method is given by,

$$(3.22) \quad \mathbf{z}_{s_{i+1}} = \mathbf{z}_{s_i} + h \left( \mathbf{I}_n - h \left( \nabla_{\mathbf{z}} \mathbf{v}^{\{\text{f}\}}(\mathbf{z}_{s_i}) \right) \right)^{-1} \mathbf{v}^{\{\text{f}\}}(\mathbf{z}_{s_i}) + \sqrt{h} \boldsymbol{\sigma}^{\{\text{s}\}}(\mathbf{z}_{s_i}) \boldsymbol{\xi},$$

where  $h = s_{i+1} - s_i$  is the time step and  $\boldsymbol{\xi} \sim \mathcal{N}(\mathbf{0}, \mathbf{I}_\ell)$ .

We now show that our proposed method is valid for solving Itô SDEs.

**THEOREM 3.3.** *A Rosenbrock Euler-Maruyama discretization for time stepping an autonomous SDE has strong order  $\mathcal{O}(h^{\frac{1}{2}})$  where  $h$  is the time step.*

*Proof.* We start with an autonomous Itô SDE in integral form given by

$$\mathbf{z}_{s_{i+1}} = \mathbf{z}_{s_i} + \int_{s_i}^{s_{i+1}} \mathbf{v}(\mathbf{z}_s) ds + \int_{s_0}^s \boldsymbol{\sigma}(\mathbf{z}_s) d\mathbf{W}_s.$$

Itô's lemma states that for any function  $f : \mathbb{R}^n \rightarrow \mathbb{R}^1$

$$f(\mathbf{z}_{s_{i+1}}) = f(\mathbf{z}_{s_i}) + \int_{s_i}^{s_{i+1}} \mathcal{D}^0(f(\mathbf{z}_s)) ds + \int_{s_0}^s \mathcal{D}^1(f(\mathbf{z}_s)) d\mathbf{W}_s,$$

where the operators  $\mathcal{D}^0$  and  $\mathcal{D}^1$  are defined as,

$$\begin{aligned} \mathcal{D}^0(f(\mathbf{z})) &= (\nabla_{\mathbf{z}} f(\mathbf{z}))^T \mathbf{v}(\mathbf{z}) + \frac{1}{2} \text{tr}(\boldsymbol{\sigma}(\mathbf{z})^T (\nabla_{\mathbf{z}}^2 f(\mathbf{z})) \boldsymbol{\sigma}(\mathbf{z})), \text{ and} \\ \mathcal{D}^1(f(\mathbf{z})) &= (\nabla_{\mathbf{z}} f(\mathbf{z}))^T \boldsymbol{\sigma}(\mathbf{z}). \end{aligned}$$

Here,  $\nabla_{\mathbf{z}}$  and  $\nabla_{\mathbf{z}}^2$  are the gradient and the Hessian respectively. Thus, for a higher dimensional function  $\mathbf{f} : \mathbb{R}^n \rightarrow \mathbb{R}^{\ell_1 \times \ell_2}$ , we have

$$\mathbf{f}(\mathbf{z}_{s_{i+1}}) = \mathbf{f}(\mathbf{z}_{s_i}) + \int_{s_i}^{s_{i+1}} \mathcal{D}^0 \odot \mathbf{f}(\mathbf{z}_s) ds + \int_{s_i}^{s_{i+1}} \mathcal{D}^1 \odot \mathbf{f}(\mathbf{z}_s) d\mathbf{W}_s.$$

Substituting the Itô-Taylor expansion of  $\mathbf{v}$  and  $\boldsymbol{\sigma}$ , we obtain

$$\mathbf{z}_{s_{i+1}} = \mathbf{z}_{s_i} + \mathbf{v}(\mathbf{z}_{s_i}) \int_{s_i}^{s_{i+1}} ds + \boldsymbol{\sigma}(\mathbf{z}_{s_i}) \int_{s_i}^{s_{i+1}} d\mathbf{W}_s + \mathcal{O}(h^{\frac{3}{2}}).$$

Discretizing with explicit Euler-Maruyama method, we get,

$$\mathbf{z}_{s_{i+1}} = \mathbf{z}_{s_i} + h \mathbf{v}(\mathbf{z}_{s_i}) + \sqrt{h} \boldsymbol{\sigma}(\mathbf{z}_{s_i}) \boldsymbol{\xi} + \mathcal{O}(h^{\frac{3}{2}}),$$

which is proven to be strong order  $\mathcal{O}(h^{\frac{1}{2}})$  [20].

In the partitioned IMEX Rosenbrock Euler-Maruyama approach, the update is split into a stiff drift component and a non-stiff diffusion component given by

$$\mathbf{z}_{s_{i+1}} = \mathbf{z}_{s_i} + h\mathbf{v}^{\{\text{f}\}} + \sqrt{h}\boldsymbol{\sigma}^{\{\text{s}\}}(\mathbf{z}_{s_i})\boldsymbol{\xi}$$

The stiff update  $\mathbf{v}^{\{\text{f}\}}$  is obtained by solving the linear system,

$$\left(\mathbf{I}_n - h\left(\nabla_{\mathbf{z}}\mathbf{v}^{\{\text{f}\}}(\mathbf{z}_{s_i})\right)\right)\mathbf{v}^{\{\text{f}\}} = \mathbf{v}^{\{\text{f}\}}(\mathbf{z}_{s_i}).$$

Observe that the new drift term is an order  $\mathcal{O}(h)$  correction to the Euler-Maruyama drift

$$\mathbf{v}^{\{\text{f}\}} = \mathbf{v}^{\{\text{f}\}}(\mathbf{z}_{s_i}) + h\left(\nabla_{\mathbf{z}}\mathbf{a}^{\{\text{f}\}}(\mathbf{z}_{s_i})\right)\mathbf{v}^{\{\text{f}\}}.$$

Which means that the full IMEX Rosenbrock Euler-Maruyama scheme,

$$\mathbf{z}_{s_{i+1}} = \mathbf{z}_{s_i} + h\mathbf{v}^{\{\text{f}\}}(\mathbf{z}_{s_i}) + h^2\left(\nabla_{\mathbf{z}}\mathbf{v}^{\{\text{f}\}}(\mathbf{z}_{s_i})\right)\mathbf{v}^{\{\text{f}\}} + \sqrt{h}\boldsymbol{\sigma}^{\{\text{s}\}}(\mathbf{z}_{s_i})\boldsymbol{\xi}$$

is an order  $\mathcal{O}(h^2)$  correction to the Euler-Maruyama scheme, preserving the strong order  $\mathcal{O}(h^{\frac{1}{2}})$  of the method, as required.  $\square$

In the VFP, the regularized drift of the Itô process (3.19) are placed into the stiff partition,  $\hat{\mathbf{v}}^{\text{f}}$  and the stochastic component  $\boldsymbol{\sigma}^{\{\text{s}\}}$  is placed in the non-stiff partition. For a chosen step-size  $h$ , the stiff update  $\mathbf{v}_s^{\{\text{f}\}}$  is calculated by solving the tensor linear system,

$$(3.23) \quad \left[\mathbf{I}_N \otimes \mathbf{I}_n - h\left(\nabla_{\mathbf{X}} \otimes \mathbf{v}^{\{\text{f}\}}(\mathbf{X}_s)\right)\right] \text{vec}\left(\mathbf{v}_s^{\{\text{f}\}}\right) = \text{vec}\left(\hat{\mathbf{v}}^{\{\text{f}\}}(\mathbf{X}_s)\right)$$

where  $\text{vec}(\cdot)$  stands for the vectorization of the vector.

By [Theorem 3.3](#), the update of the system from pseudo-time  $s_i$  to  $s_{i+1}$

$$(3.24) \quad \mathbf{X}_{s_{i+1}} = \mathbf{X}_{s_i} + h\mathbf{v}_s^{\{\text{f}\}} + \sqrt{h}\boldsymbol{\sigma}_s^{\{\text{s}\}}(\mathbf{X}_{s_i})\boldsymbol{\xi},$$

under the IMEX Rosenbrock Euler-Murayama scheme.

**REMARK 7.** *Rather than calculate a full tensor Jacobian  $\nabla_{\mathbf{X}} \otimes \mathbf{v}^{\{\text{f}\}}(\mathbf{X}_s)$ , it is memory efficient to work with Jacobian vector products. In a lot of problems, it maybe more feasible to obtain a finite difference approximation to the Jacobian vector product than calculating an analytical Jacobian vector product. For more on this see [38]. Additionally, since Rosenbrock-Euler is a W method [36] the Jacobian need not be calculated accurately, and can be kept constant for multiple steps or have missing parts. These methods can however be impractical for large systems, thus, this is still an open problem.*

**REMARK 8.** *The time-stepping problem (3.21) can be seen as an optimization problem. Methods for performing stochastic optimization such as ADAM [19] can also be used as alternatives to the scheme provided herein.*

**3.5. Flavors of the variational Fokker-Planck filters and smoothers.** As noted in [subsection 3.2](#), the drift term (3.11) in the VFP can be fully described by the choice of parameterization of the prior and intermediate distribution along with

the (assumed to be known) distribution of the observations. We next provide several examples of gradient log-likelihoods of the analysis and intermediate distributions.

For a given realization  $\mathbf{y}$  of the observation (2.1), we discuss several possible gradient log-likelihoods. We first discuss the case of unbiased Gaussian observation error (see Table 3.1), the gradient log-likelihood is given by,

$$(3.25) \quad \nabla_{\mathbf{x}} \log \pi_o(\mathbf{x}) = -\mathbf{H}^T \mathbf{R}^{-1} (\mathcal{H}(\mathbf{x}) - \mathbf{y})$$

where  $\mathbf{R}$  is the observation error covariance, and  $\mathbf{H}^T$  is the adjoint of the observation operator  $\mathcal{H}$ .

By (3.14) and under Gaussian assumptions (see Table 3.1) on the prior and intermediate distributions, the drift term (3.11) with Gaussian observations (3.25) can be written as,

$$(3.26) \quad \begin{aligned} \mathbf{v}(\mathbf{X}_s) = & -\mathbf{P}_f^{-1} (\mathbf{X}_s - \bar{\mathbf{x}}_f) - \mathbf{H}^T \mathbf{R}^{-1} (\mathcal{H}(\mathbf{X}_s) - \mathbf{y}) \\ & - (\mathbf{D}(\mathbf{X}_s) - \mathbf{I}_n) \mathbf{P}_s^{-1} (\mathbf{X}_s - \bar{\mathbf{x}}_s) + (\nabla_{\mathbf{x}}^T \mathbf{D}(\mathbf{X}_s))^T, \end{aligned}$$

where from (2.7),  $\mathbf{P}_f$  and  $\mathbf{P}_s$  are the forecast ensemble and intermediate ensemble covariances, respectively, and, similarly,  $\bar{\mathbf{x}}_f$  and  $\bar{\mathbf{x}}_s$  are the means. As discussed in subsection 3.2, this approach is termed VFP(GG) to denote the Gaussian assumptions on the prior and intermediate distributions respectively.

With unbiased (in mode) Cauchy observation error (see Table 3.1), the gradient log-likelihood is given by

$$(3.27) \quad \nabla_{\mathbf{x}} \log \pi_o(\mathbf{x}) = -\frac{n+1}{1 + (\mathcal{H}(\mathbf{x}) - \mathbf{y})^T \mathbf{R}^{-1} (\mathcal{H}(\mathbf{x}) - \mathbf{y})} \mathbf{H}^T \mathbf{R}^{-1} (\mathcal{H}(\mathbf{x}) - \mathbf{y}),$$

and the drift term (3.11) in the VFP(GG) approach (3.26) is correspondingly modified to be

$$(3.28) \quad \begin{aligned} \mathbf{v}(\mathbf{X}_s) = & -\mathbf{P}_f^{-1} (\mathbf{X}_s - \bar{\mathbf{x}}_f) \\ & - \frac{n+1}{1 + (\mathcal{H}(\mathbf{x}) - \mathbf{y})^T \mathbf{R}^{-1} (\mathcal{H}(\mathbf{x}) - \mathbf{y})} \mathbf{H}^T \mathbf{R}^{-1} (\mathcal{H}(\mathbf{x}) - \mathbf{y}), \\ & - (\mathbf{D}(\mathbf{X}_s) - \mathbf{I}_n) \mathbf{P}_s^{-1} (\mathbf{X}_s - \bar{\mathbf{x}}_s) + (\nabla_{\mathbf{x}}^T \mathbf{D}(\mathbf{X}_s))^T \end{aligned}$$

where  $\mathbf{R}$  is a measure of scale in the Cauchy distribution.

We provide one last example of a filter in the VFP framework under Laplace assumptions on the prior and Gaussian assumptions on the intermediate distribution (see Table 3.1), which we name the VFP(LG). Again taking unbiased Gaussian observation error (3.25), we arrive at the following drift term (3.11),

$$(3.29) \quad \begin{aligned} \mathbf{v}(\mathbf{X}_s) = & -\frac{2}{\theta_f} \frac{\mathcal{K}_{\nu-1}(\theta_f)}{\mathcal{K}_{\nu}(\theta_f)} \mathbf{P}_f^{-1} (\mathbf{X}_s - \bar{\mathbf{x}}_f) - \mathbf{H}^T \mathbf{R}^{-1} (\mathcal{H}(\mathbf{X}_s) - \mathbf{y}) \\ & - (\mathbf{D}(\mathbf{X}_s) - \mathbf{I}_n) \mathbf{P}_s^{-1} (\mathbf{X}_s - \bar{\mathbf{x}}_s) + (\nabla_{\mathbf{x}}^T \mathbf{D}(\mathbf{X}_s))^T, \end{aligned}$$

where  $\theta_f$  is a term related to the mean and covariance of the prior distribution.

The VFP can also handle smoothing (2.4) observation distributions, where a window of observations is assimilated all at once. Following (3.15), a Gaussian smoothing observation distribution coupled with a Gaussian assumption on the prior, begets the following gradient log-likelihood at time  $t_i$ ,

$$(3.30) \quad \nabla_{\mathbf{x}} \log \pi_a = -\mathbf{P}_f^{-1} (\mathbf{X}_s - \bar{\mathbf{x}}_f) - \sum_{k=1}^K \mathbf{H}_{i+k}^T \mathbf{M}_{i \rightarrow i+k}^T \mathbf{R}_k^{-1} (\mathcal{H}_{i+k}(\mathcal{M}_{i \rightarrow i+k}(\mathbf{X}_s)) - \mathbf{y}_{i+k}),$$

where  $\mathbf{M}^T$  is the adjoint of the model operator (2.3), and  $\mathbf{y}_{i+k}$  are the observations at future times. We can derive a drift term (3.11) for this approach,

$$(3.31) \quad \begin{aligned} \mathbf{v}(\mathbf{X}_s) = & -\mathbf{P}_f^{-1}(\mathbf{X}_s - \bar{\mathbf{x}}_f) \\ & - \sum_{k=1}^K \mathbf{H}_{i+k}^T \mathbf{M}_{i \rightarrow i+k}^T \mathbf{R}_k^{-1} (\mathcal{H}_{i+k}(\mathcal{M}_{i \rightarrow i+k}(\mathbf{X}_s)) - \mathbf{y}_{i+k}), \\ & - (\mathbf{D}(\mathbf{X}_s) - \mathbf{I}_n) \mathbf{P}_s^{-1} (\mathbf{X}_s - \bar{\mathbf{x}}_s) + (\nabla_{\mathbf{x}}^T \mathbf{D}(\mathbf{X}_s))^T \end{aligned}$$

under Gaussian assumptions on the intermediate distribution. We term the VFP smoother as the VFPS, name the approach in (3.31) as the VFPS(GG).

REMARK 9. *It is clear from (3.30) that the logarithm of the posterior is exactly the same as the 4D-Var gradient. Subtracting  $-\mathbf{P}_s^{-1}(\mathbf{X}_s - \bar{\mathbf{x}}_s)$  can be viewed as a regularizing term that pushes each particle away from the intermediate mean of  $\mathbf{X}_s$ . The variational Fokker-Planck smoother with Gaussian assumptions can be thought of as a regularized ensemble 4D-Var, however, there is no strict requirement for any of the distributions to be necessarily Gaussian.*

We next provide several trivial numerical examples to highlight the VFP approach.

**3.5.1. Demonstration of regularization and diffusion.** For the first demonstration, we look at the effects of the diffusion component in the Itô process (3.10) and the regularization component in the augmented drift (3.19), as applied to a simple ensemble.

We aim to analyze the difference between four different methods with Gaussian and Laplace assumptions on the prior and intermediate distributions (see Table 3.1). We analyze VFP(GG), VFP(GL), VFP(LG), and VFP(LL) where the first letter represents the prior assumption and the second the intermediate assumption.

Four sets of prior ensembles are taken, coupled with a simple Gaussian observation, and evolved through the ensemble Itô process (3.10).

Three experiments are performed (i) assimilation in the absence of both diffusion and regularization, (ii) assimilation in the presence of diffusion only, (iii) assimilation in the presence of regularization only. The results of these experiments can be seen in Figure 3.1, with the prior ensembles described by Figure 3.1a.

Without diffusion or regularization Figure 3.1b, VFP(LG) and VFP(LL) suffer from ensemble collapse in one step. The fully Gaussian VFP(GG) has a diverse set of samples both close to and far away from the mean, while VFP(GL) forms a ring around the mean.

With the addition of diffusion in Figure 3.1c, all the ensembles have a diverse set of particles both close to and far from the analysis means. The ensembles of VFP(LG) and VFP(LL) no longer suffer from ensemble collapse, and the ensemble of VFP(GL) shows a much weaker ring-like structure. The ensemble of VFP(GG) does not seem to have any qualitative difference as opposed to that without diffusion.

With the addition of regularization in Figure 3.1d, all the particles seem to have much more uniform distribution along their support, with each method having its own unique circle-like structure. The problematic methods VFP(LG) and VFP(LL) still seem to suffer from ensemble collapse, VFP(GL) still preserves a distinct ring-like structure around the whole ensemble, and VFP(GG) seems like non-independent sampling.

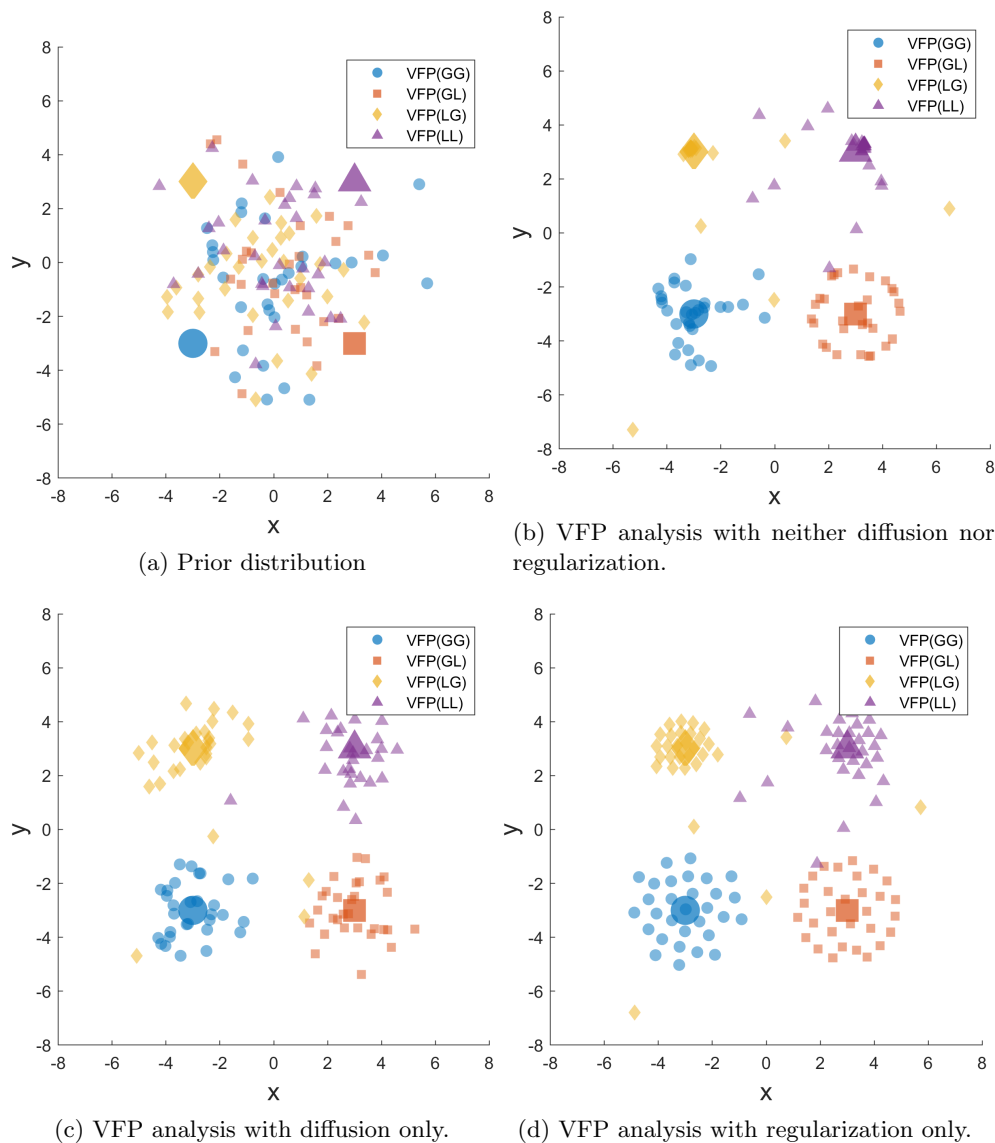


Fig. 3.1: Comparison of the ensemble distributions by augmenting the four flavors VFP, namely VFP(GG), VFP(GL), VFP(LG), and VFP(LL), with diffusion and regularization strategies. The four large symbols represent the means of the four analysis distributions and the smaller symbols represent the analysis particles.

From these results we are able to ascertain that both diffusion and regularization play important roles in achieving optimal ensemble-based inference.

**3.5.2. Demonstration of multimodal assimilation.** We now show on a simple one dimensional example how the VFP can be utilized for multimodal data assimilation.

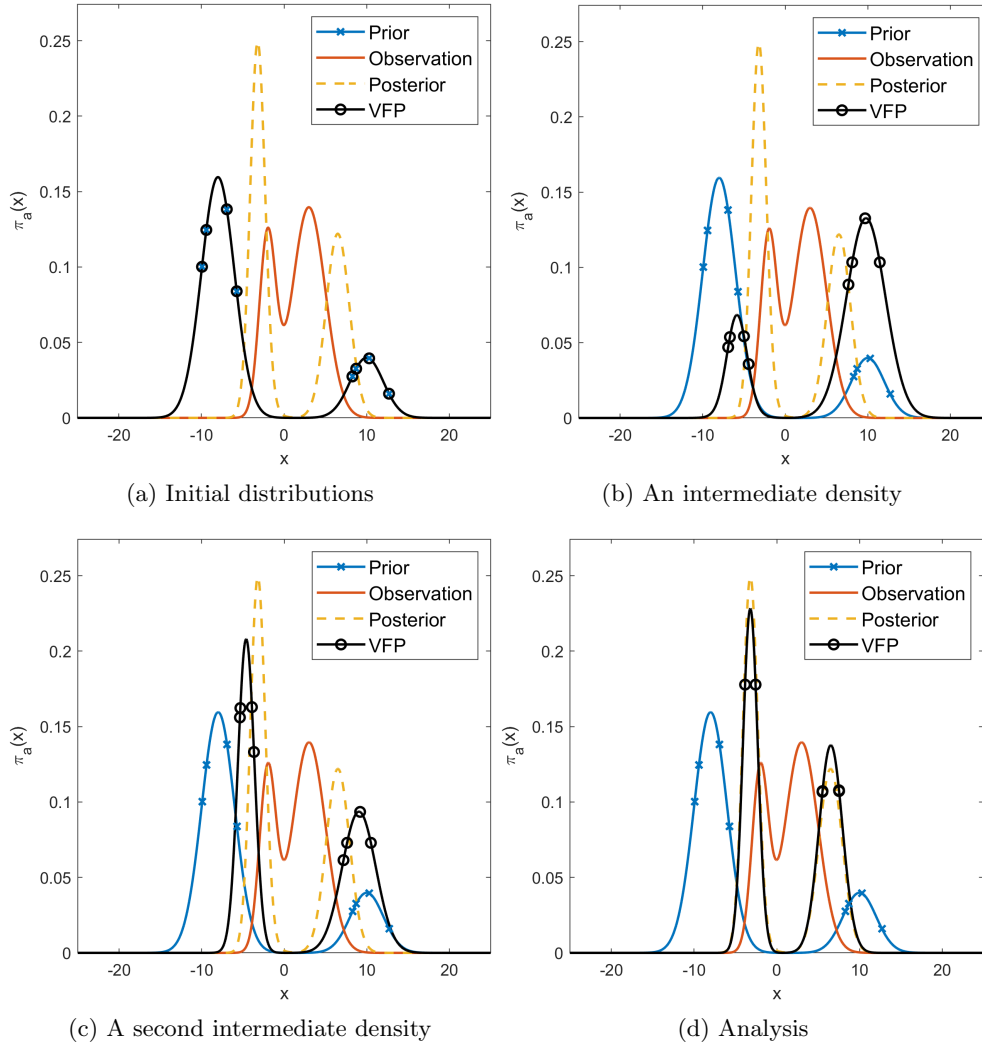


Fig. 3.2: This example compares the analysis for a Gaussian mixture. Though there are 4 modes, the 2 weak modes get subsumed by the 2 dominant modes in both the exact posterior and our analysis.

Let the prior distribution have  $M_f$  modes and the observation distribution  $M_o$  modes. Then, the posterior must have at most  $M_f \times M_o$  modes, which in practice is much lesser as many weaker modes get subsumed by stronger modes.

For assimilation, the prior ensemble is first clustered into its  $M_f$  sub-ensembles, each of which are further divided into  $M_o$  different sub-sub-ensembles. Each sub-sub-ensemble performs assimilation in a parallel fashion for its respective prior and observation distributions. When all sub-sub-ensembles have completed assimilation, we have the ensemble analysis.

However, to reconstruct the optimal analysis distribution, it must be stitched together in a specific fashion. First, weights are estimated for each analysis particle

to be equal to their observational likelihood,

$$(3.32) \quad \mathbf{w} = \pi_o(\mathbf{X}_a).$$

The total weight for each sub-sub-ensemble is calculated by adding the weights of all the particles within that sub-sub-ensemble,

$$(3.33) \quad \mathbf{w}_{i,j} \propto \sum \mathbf{w}, \quad i = 1, \dots, M_f, \quad j = 1, \dots, M_o,$$

with the weights for each sub-sub-ensemble normalized by their sum to have the total weight of the full ensemble equal to one.

Based on the distribution assumption, the analysis distribution is calculated as a weighted sum of every sub-sub-analysis distribution where the weights come from the aforementioned calculation in (3.33) and the distribution is assumed in a parameterized sense. Though this approach can be extended to high dimensional problems, it is an open question if this is the best approach to multimodal analysis under the VFP framework.

In Figure 3.2, we assume a bimodal Gaussian mixture prior and a bimodal observation distribution in a one-dimensional setting and perform one assimilation step using VFP(GG). Though there is a slight discrepancy between the exact posterior distribution and the constructed analysis, each of the dominant modes are accurately captured.

**3.6. Localization and Covariance Shrinkage.** As the prior and intermediate distributions are parameterized, certain assumptions on the distributions require the online estimation of the covariance matrix. In high dimensional systems, when  $N \ll n$ , the estimated low-rank covariance has spurious correlations between the states. In most systems of interest, which are spatially-defined, the correlations between any two states is inversely proportional to their distance. The VFP formulation permits the usage of localization and covariance shrinkage to ameliorate the issues with covariance estimation.

**3.6.1. Local Update with Schur-product Localization.** Schur-product localization [3, 26] corrects the covariance estimate by performing an element-wise product of the covariance  $\mathbf{P}$  with a decorrelation matrix  $\mathbf{C}$  that is a function of the distances between the states. Let  $d(i, j)$  be a metric between the  $i$ th and  $j$ th states of the system. Then, the covariance estimate is given by,

$$(3.34) \quad \mathbf{P}_{\text{loc}} = \mathbf{P} \circ \mathbf{C}, \quad \text{where } \mathbf{C}_{i,j} = \rho\left(\frac{d(i,j)}{r}\right),$$

where,  $\rho(\zeta)$  is a chosen decorrelation function and  $r$  is the decorrelation radius.

In the local-update approach to localization, each  $i$ th state variable is updated independently with the principle symmetric positive definite submatrix,

$$(3.35) \quad \mathbf{P}_{\text{loc},i} = \mathbf{D} \circ \mathbf{P}_{\text{loc}}, \quad \text{where } \mathbf{D}_{j,k} = \begin{cases} \rho\left(\frac{d(i,j)}{r}\right), & j = k \\ 0, & \text{otherwise} \end{cases},$$

acting locally on the non-zero variance states. This dual-combination localization will be utilized in this work.

Popular choices for the decorrelation function are the Gaussian and the piecewise rational Gaspari-Cohn [13] with compact support. The decorrelation function used

in this work is the Gaspari-Cohn given by.

$$(3.36) \quad \rho(\zeta) = \begin{cases} -\frac{1}{4} \left(\frac{\zeta}{\theta}\right)^5 + \frac{1}{2} \left(\frac{\zeta}{\theta}\right)^4 + \frac{5}{8} \left(\frac{\zeta}{\theta}\right)^3 - \frac{5}{3} \left(\frac{\zeta}{\theta}\right)^2 + 1 & 0 \leq \zeta \leq \theta, \\ \frac{1}{12} \left(\frac{\zeta}{\theta}\right)^5 - \frac{1}{2} \left(\frac{\zeta}{\theta}\right)^4 + \frac{5}{8} \left(\frac{\zeta}{\theta}\right)^3 + \frac{5}{3} \left(\frac{\zeta}{\theta}\right)^2 - 5 \left(\frac{\zeta}{\theta}\right) + 4 - \frac{2}{3} \left(\frac{\theta}{\zeta}\right) & \theta < \zeta \leq 2\theta, \\ 0 & \text{otherwise,} \end{cases}$$

with an optimally chosen parameter  $\theta$ . Since the Gaspari-Cohn function has compact support, the decorrelation matrix  $\mathbf{C}$  will be sparse.

**3.6.2. Covariance Shrinkage.** When the analysis and intermediate distributions in the drift (3.11) are assumed Gaussian Table 3.1, covariance shrinkage methods [6] can be used to correct the covariance. In this work, the Rao-Blackwell Ledoit-Wolf shrinkage estimator is specifically used. For a Gaussian ensemble  $\mathbf{X} \in \mathbb{R}^{n \times N}$ , the shrinkage covariance,

$$(3.37) \quad \mathbf{P}_{\text{RBLW}} = (1 - \gamma)\mathbf{P} + \gamma\hat{\Sigma}$$

$$(3.38) \quad \gamma = \min \left( \frac{\left[ \frac{N-2}{N} \text{tr}(\mathbf{P}^2) \right] + \text{tr}^2(\mathbf{P})}{(N+2) \left[ \text{tr}(\mathbf{P}^2) - \frac{\text{tr}^2(\mathbf{P})}{n} \right]}, 1 \right)$$

can be utilized, where the  $\mathbf{P}$  is covariance of samples, and the target covariance  $\hat{\Sigma}$ ,

$$(3.39) \quad \hat{\Sigma} = \frac{\text{tr}(\mathbf{P})}{n} \mathbf{I}_n,$$

is chosen to be the trace-normalized identity.

**4. Numerical Experiments.** We now illustrate the effectiveness of the VFP as opposed to other state-of-the-art methods with a few numerical experiments. One of the metrics that we will utilize is spatio-temporal RMSE. Spatio-temporal RMSE is calculated as

$$(4.1) \quad \text{RMSE} = \sqrt{\frac{1}{nT} \sum_{k=1}^T \sum_{i=1}^n ([\mathbf{x}_{\text{true},k}]_i - [\bar{\mathbf{x}}_{a,k}]_i)^2}$$

where  $T$  represents every assimilation step post spinup, and  $\bar{\mathbf{x}}_{a,k}$  is the analysis mean at the  $k$ th time-step.

All test problems and implementations were taken from the ODE Test problems suite [8, 33].

**4.1. Lorenz '63.** For our first round of experiments, we use the canonical 3-variable Lorenz '63 model [25],

$$(4.2) \quad \frac{dx}{dt} = \sigma(y - x), \quad \frac{dy}{dt} = x(\rho - z) - y, \quad \frac{dz}{dt} = xy - \beta z,$$

to showcase various properties of our formulation. We set the parameters in (4.2) to their canonical values of  $\sigma = 10$ ,  $\rho = 28$ ,  $\beta = \frac{8}{3}$ .

The model is assumed to be exact, and is propagated in time using the Dormand-Prince 5(4) method [9]. The following Lorenz '63 experiments are run for 55000 steps ignoring statistics from the 5000 as spinup. Each experiment is repeated 12 times

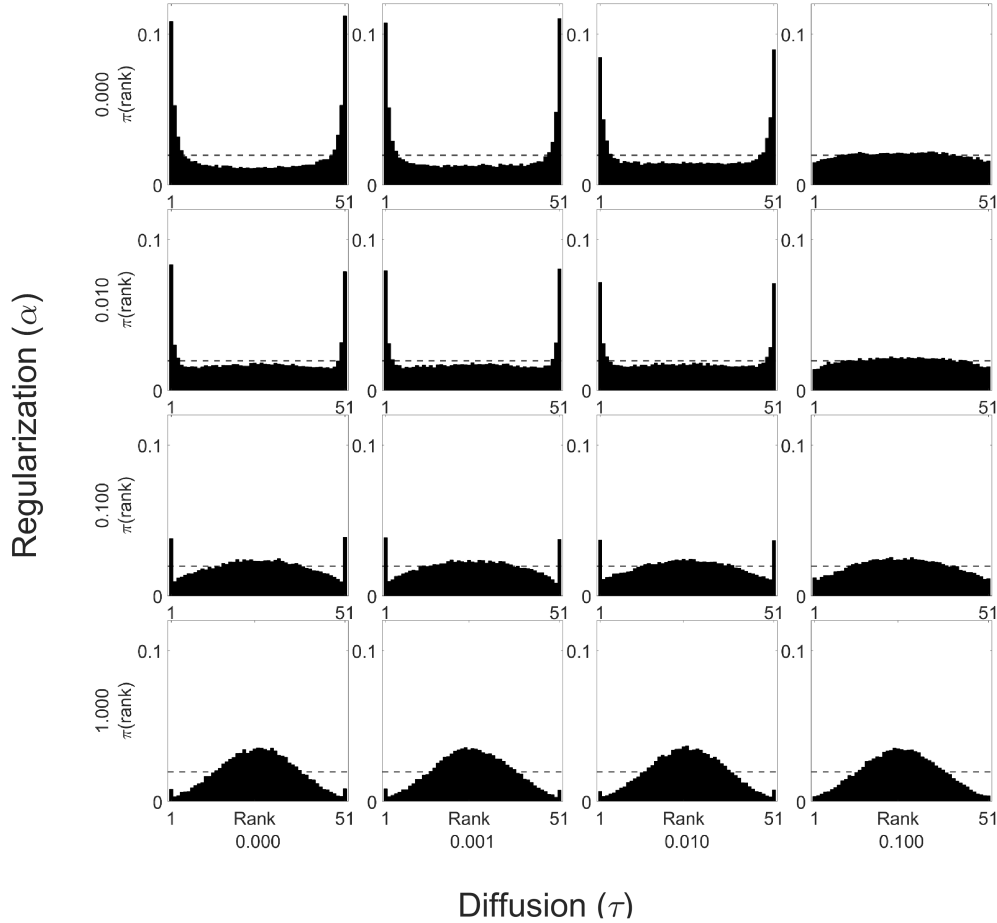


Fig. 4.1: Rank histograms for 50 particles obtained at different parameter values of the diffusion parameter  $\tau$  and the regularization parameter  $\alpha$ . The ideal parameter choice is the one that gives a uniform rank histogram.

with different random seeds with the results averaged to ensure robustness. The observations are assimilated every  $\Delta t = 0.12$ , which is equivalent to an atmospheric time scale of 9 hours [37]. We observe all three variables with either unbiased Gaussian error with covariance  $\mathbf{R} = 8\mathbf{I}_3$ , or with Cauchy observation error with  $\mathbf{R} = \mathbf{I}_3$ . Each experiment is repeated 12 times with different random seeds with the results averaged to ensure robustness.

**4.1.1. Effect of diffusion and regularization on an ensemble rank histogram.** In this first experiment we wish to analyze the quality of the analysis ensemble by varying the diffusion and regularization coefficients.

Rank histograms [14] evaluate the accuracy of ensemble predictions by analyzing the error with the ensemble mean and spread. A good ensemble prediction method is one that has a uniform rank histogram. In our experiment, a rank histogram of the first variable of the analysis is constructed with the true trajectory taken as the reference.

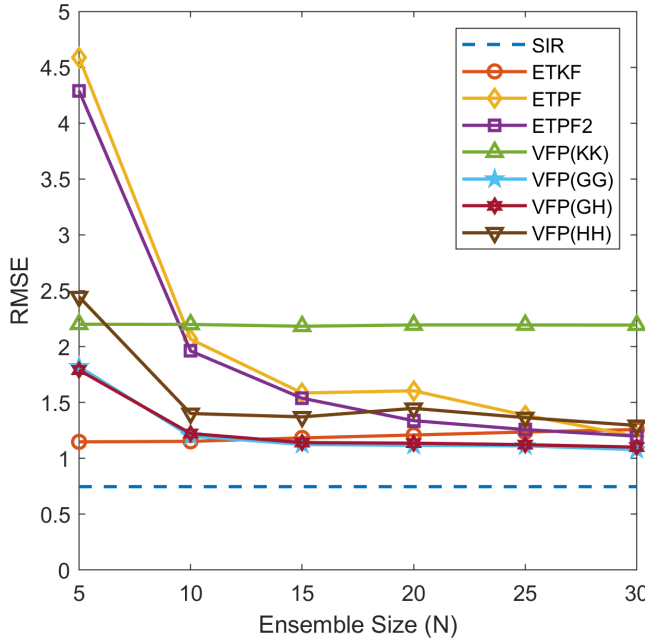


Fig. 4.2: Variation in the ensemble size as compared to the analysis RMSE for various VPF methods and the ETKF, ETPF and SIR baseline, with a Gaussian observation covariance of  $\mathbf{R} = 8\mathbf{I}_3$ .

For diffusion we take,

$$(4.3) \quad \sigma(X_s) = \tau \mathbf{A}_f,$$

where  $\mathbf{A}_f$  are the scaled forecast ensemble anomalies defined by (2.7), and  $\tau$  is a parameter. For regularization we use the electrostatic force (3.20) with  $\alpha$  as the parameter.

The VFP(GG) method is used as the assimilation scheme with the noisy Gaussian unbiased error covariance of  $8\mathbf{I}_3$ , and an ensemble size of  $N = 50$ . The parameters are varied as follows:  $\tau = \{0, 0.001, 0.01, 0.1\}$  and  $\alpha = \{0, 0.01, 0.1, 1\}$ .

Figure 4.1 provided a visual overview of the results of this experiment. It is clear that for a low and high values of the regularization parameter  $\alpha$ , the rank histogram tends away from a uniform distribution. For diffusion on the other hand, the higher the value, the more uniform the rank histogram becomes.

Based on Figure 4.1, we choose  $\tau = 0.1$  and  $\alpha = 0.01$  for the subsequent experiments on the Lorenz '63 system, with the caveat that these values may be optimal only for this particular setting.

**4.1.2. Gaussian Observation Error.** We use the standard experimental setup with a linear observation operator  $\mathcal{H}(\mathbf{x}) = \mathbf{x}$  and unbiased Gaussian observation error covariance  $R = 8\mathbf{I}_3$ . We modify the ensemble size  $N$  and observe the analysis RMSE (4.1) for each one.

We present 4 different formulations of the variational Fokker-Planck, namely, the VFP(GG), VFP(GH), VFP(HH), and VFP(KK) schemes (see Table 3.1 for more details about the distributions underlying these assumptions). For the Huber dis-

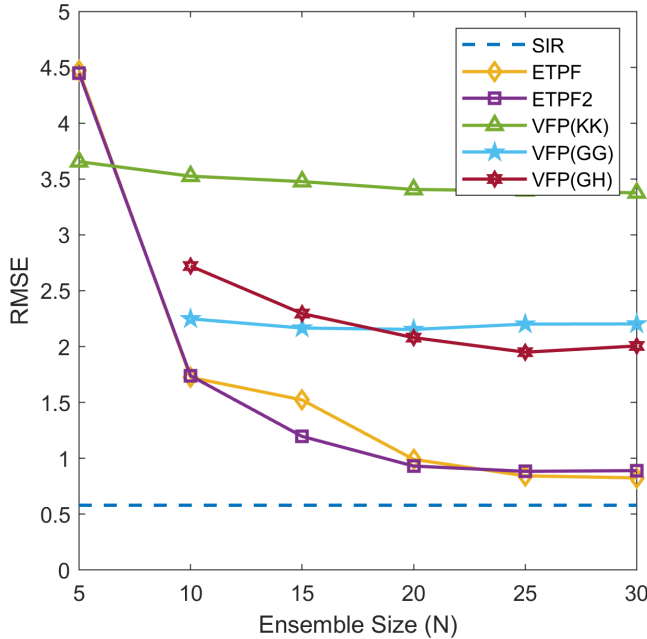


Fig. 4.3: Cauchy observation with scale  $\mathbf{R} = \mathbf{I}_3$

tribution parameters we choose  $\delta_1 = \delta_2 = 1$  based on empirical performance. The VFP(KK) scheme will serve in the place of the MPF, as they are nearly identical in form and function, with the Kernel covariance parameter computed in a similar fashion to [29]. These schemes will be compared to the ETKF (with an optimal inflation for each ensemble size  $N$ ), ETPF and the second order accurate ETPF (ETPF2). For the baseline theoretical lower-bound error the sequential importance resampling particle filter (SIR) with an ensemble size of  $N = 10000$  particles is utilized, as in the limit  $N \rightarrow \infty$  it performs exact Bayesian inference. The analysis RMSE for this line of experiments can be seen in Figure 4.2 for various ensemble sizes  $N$ .

The VFP(GG) and ETKF both approximate fully-Gaussian inference and can be seen as different discretizations of the Kalman filter, thus it is not surprising that their performance is the same. The VFP(HH) shows a slightly higher RMSE, which may be due to the fact that the underlying Laplace distribution is super-Gaussian, while the support of the dynamics of the system is sub-Gaussian [41]. The VFP(KK) has poor performance, meaning that the MPF would likely also perform poorly on this problem formulation.

**4.1.3. Cauchy Observation Error.** The settings for this experiment are the same as the Lorenz '63 with Gaussian observations in subsection 4.1.2, except for the observation distribution, which is set to the Cauchy distribution with scale parameter  $\mathbf{R} = \mathbf{I}_3$ . The analysis RMSE for this line of experiments can be seen in Figure 4.3 for various ensemble sizes  $N$ .

The ETKF fails to converge for any observation covariance choice as the distribution of the observations is non-Gaussian. The VFP(HH) also fails to converge.

The VFP(KK) (and likely the MPF) performs really poorly for these given settings, likely because of poor choices for the Kernel covariances.

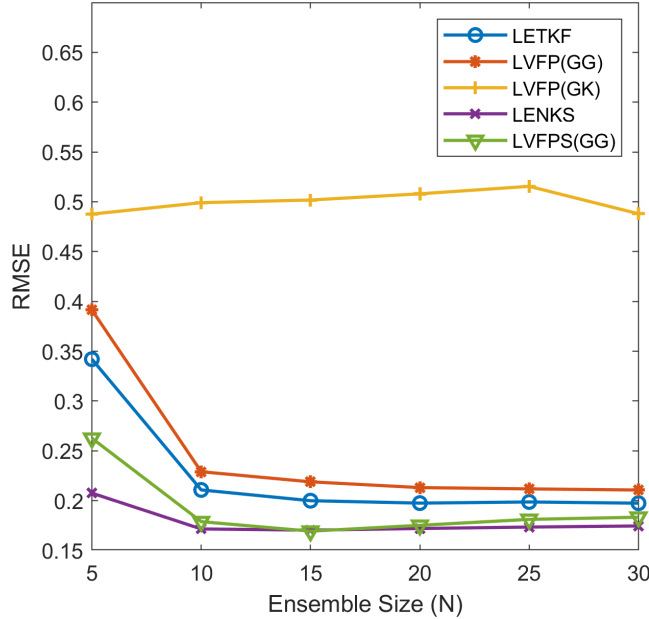


Fig. 4.4: For the Lorenz '96 equations ensemble size  $N$  is compared to the analysis RMSE. Various localized VFP filters and a smoother are compared to the standard LETKF and LETKS.

The VFP(GG) and VFP(GH) perform similarly well, with the VFP(GH) performing slightly better likely because of the slight super-Gaussianity of the Huber distribution being more similar to the Cauchy distribution of the observations.

Although some of the VFP methods perform better than the purely Gaussian ETKF, they still perform worse than the purely non-Gaussian ETPF family of methods. This leads us to conclude that the VFP can act as a bridge between Gaussian filtering and non-Gaussian filtering.

**4.2. Lorenz '96.** The next experiment is performed on the 40-variable Lorenz '96 problem [24, 39] given by

$$(4.4) \quad \frac{dx_i}{dt} = (x_{i+1} - x_{i-2})x_{i-1} - x_i + F, \quad \text{for } i = 1, \dots, 40 \quad \text{and } F = 8,$$

where the cyclic boundary conditions  $x_{-1} = x_{39}$ ,  $x_0 = x_{40}$  and  $x_{41} = x_1$  apply.

The Dormand-Prince 5(4) is used for time-stepping the dynamical system with a time span of  $\Delta t = 0.05$  which corresponds to six hours in real time. We assimilate for 2200 cycles discarding the first 200. The experiment is averaged over 12 different random seeds. We observe all variables with the linear observation operator  $\mathcal{H}(\mathbf{x}) = \mathbf{x}$  along with the unbiased Gaussian error covariance  $\mathbf{R} = \mathbf{I}_{40}$ .

The diffusion and regularization are chosen as  $\tau = 1e - 1$  and  $\alpha = 0$ .

We will look at three different localized (see subsection 3.6.1) versions of the VFP filters and smoothers, a localized Gaussian prior Gaussian intermediate filter LVFP(GG), a localized Gaussian prior Kernel intermediate filter LVFP(GK), and a localized variant of (3.31) which is a Gaussian prior Gaussian intermediate smoother

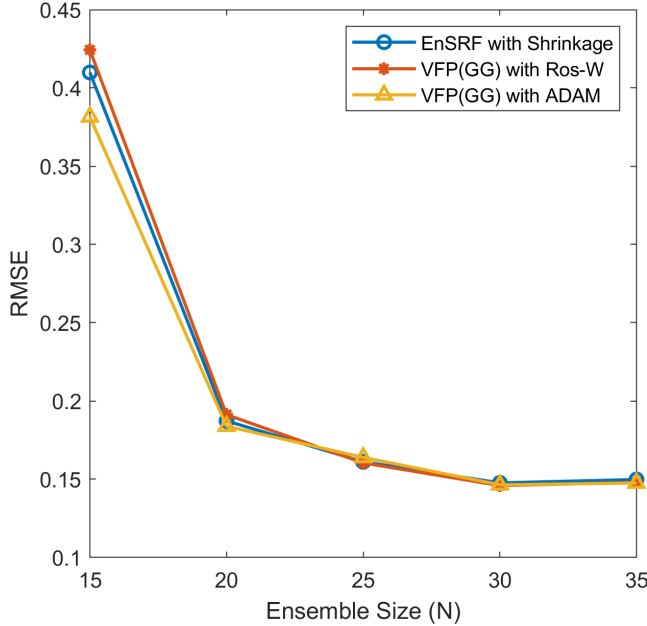


Fig. 4.5: A comparison of a Shrinkage-based ensemble Kalman filter with the shrinkage-based VFP(GG) algorithm. The VFP solution is obtained by two time-stepping algorithms, the IMEX Rosenbrock Euler-Maruyama, and the ADAM stochastic optimization scheme. As usual, ensemble size  $N$  is compared to the analysis RMSE.

LVFPS(GG). While Schur-localization is performed on the LVFPS(GG), local update is not. The LVFP(GK) is a variant of the particle flow filter (PFF) introduced in [16].

We compare the VFP methods to the localized ensemble transform Kalman filter (LETKF) [17], and a localized ensemble transform Kalman smoother LETKS [4]. The Gaspari-Cohn decorrelation function (3.36) with a radius of 4 units is used for all localization. For the smoothers, a look-ahead window of  $K = 5$  is considered.

We compared several different ensemble sizes  $N$  to the analysis RMSE. The results of these experiments are shown in Figure 4.4. The two Gaussian filters, the LVFP(GG) and the LETKF, have very similar performance. Likewise, the two smoothers, the LVFPS(GG) and LETKS also have similar performance. The particle flow filter LVFP(GK), however, had significantly higher errors for this problem setup.

**4.3. Quasi-Geostrophic equations.** The quasi-geostrophic equations [35] approximate oceanic and atmospheric dynamics where the Coriolis and pressure gradient forces are almost balanced. The PDE can be written as,

$$(4.5) \quad \begin{aligned} \omega_t + \mathbf{J}(\psi, \omega) - Ro^{-1}\psi_x &= Re^{-1}\Delta\omega + Ro^{-1}\mathbf{F}, \\ \mathbf{J}(\psi, \omega) &\equiv \psi_y\omega_x - \psi_x\omega_y, \quad \mathbf{F} = \sin(\pi(y-1)), \quad \omega = -\Delta\psi \end{aligned}$$

where  $\omega$  is the vorticity,  $\psi$  is the streamfunction,  $Re = 450$  is the Reynolds number,  $Ro = 0.0036$  is the Rossby number,  $\mathbf{J}$  is the non-linear Jacobian, and  $\mathbf{F}$  is the symmetric double gyre forcing term. The domain is defined to be  $\Omega = [0, 1] \times [0, 2]$  which is discretized on a  $63 \times 127 = 8001$  grid. The homogeneous Dirichlet boundary condition

of  $\psi_{\partial\Omega} = 0$  is assumed for all time. Our results consider the spatio-temporal RMSE for 400 steps discarding the first 50 as spinup, averaged over 12 different random seeds.

Observations are assimilated every  $\Delta t = 0.0109$  time units that is approximately one day in the atmospheric time scale. We observe 150 evenly spaced states between 1 and 8001 with the Gaussian observation error covariance being  $\mathbf{R} = \mathbf{I}_{150}$ .

We perform assimilation with our method VFP(GG) with RBLW shrinkage on the covariance estimates. We also wish to compare the performance of the time stepping procedure introduced in [Theorem 3.3](#) to that of the ADAM stochastic optimization procedure (see [Remark 8](#)). [Figure 4.5](#) shows that the VFP methods show similar performance compared to a shrinkage based left transform ensemble square root filter [\[4\]](#).

**5. Conclusion.** We provide a generalization of several methods that have been developed over the past few years. We combine the ideas of Fokker-Planck-based data assimilation [\[32\]](#) with the parameterized distribution approaches to particle flow presented in [\[16, 29\]](#). We show that the Mapping Particle Filter and the Particle Flow Filter are all methods of this generalized framework, and provide a unified codification and language by which future methods in these families can be described. Our formulation allows for flexibility in the choice of distributions while at the same time, competing with traditional methods such as ETKF, and ETPF.

We extend the idea of particle flow filtering to particle flow smoothing, and show that this approach is comparable to other state-of-the-art smoothing methods. We show that our methodology works well on low-dimensional systems as well as high dimensional problems that mimic atmospheric dynamics. Our methodology provides theoretical ways in which rejuvenation and regularization can be formalized in particle flow filters, and paves the way for a rejection of heuristics in favor of robust theory.

Additionally we have developed a robust implicit-explicit scheme by which Fokker-Planck-based particle flow filters can be integrated in pseudo-time, increasing the operational viability of these methods. Though this method allows the usage of relatively larger time-steps than fully explicit counterparts, the Jacobian vector product can become computationally expensive in higher dimensions.

Choosing optimal parameterized distributions for the forecast and intermediate such that they are closer to particle filtering philosophy is an important research direction as high dimensional problems are not flexible with the choice of parameterized distribution. Further research exploring parameterized families especially kernel-based distributions is necessary. An interesting research direction we plan to explore in a future work is momentum methods to evolve the Itô process.

#### REFERENCES

- [1] W. ACEVEDO, J. DE WILJES, AND S. REICH, *Second-order accurate ensemble transform particle filters*, SIAM Journal on Scientific Computing, 39 (2017), pp. A1834–A1850, <https://doi.org/10.1137/16M1095184>, <https://doi.org/10.1137/16M1095184>, <https://arxiv.org/abs/https://doi.org/10.1137/16M1095184>.
- [2] J. L. ANDERSON, *A marginal adjustment rank histogram filter for non-gaussian ensemble data assimilation*, Monthly Weather Review, 148 (01 Aug. 2020), pp. 3361 – 3378, <https://doi.org/10.1175/MWR-D-19-0307.1>, <https://journals.ametsoc.org/view/journals/mwre/148/8/mwrD190307.xml>.
- [3] J. L. ANDERSON, *Exploring the need for localization in ensemble data assimilation using a hierarchical ensemble filter*, Physica D: Nonlinear Phenomena, 230 (2007), pp. 99–111, <https://doi.org/https://doi.org/10.1016/j.physd.2006.02.011>, <https://www>.

- sciencedirect.com/science/article/pii/S0167278906002168. Data Assimilation.
- [4] M. ASCH, M. BOCQUET, AND M. NODET, *Data Assimilation*, Society for Industrial and Applied Mathematics, Philadelphia, PA, 2016, <https://doi.org/10.1137/1.9781611974546>, <https://epubs.siam.org/doi/abs/10.1137/1.9781611974546>, <https://arxiv.org/abs/https://epubs.siam.org/doi/pdf/10.1137/1.9781611974546>.
  - [5] G. BURGERS, P. J. VAN LEEUWEN, AND G. EVENSEN, *Analysis scheme in the ensemble kalman filter*, Monthly Weather Review, 126 (1998), pp. 1719 – 1724, [https://doi.org/10.1175/1520-0493\(1998\)126\(1719:ASITEK\)2.0.CO;2](https://doi.org/10.1175/1520-0493(1998)126(1719:ASITEK)2.0.CO;2), [https://journals.ametsoc.org/view/journals/mwre/126/6/1520-0493\\_1998\\_126\\_1719\\_asitek\\_2.0.co\\_2.xml](https://journals.ametsoc.org/view/journals/mwre/126/6/1520-0493_1998_126_1719_asitek_2.0.co_2.xml).
  - [6] Y. CHEN, A. WIESEL, Y. C. ELGAR, AND A. O. HERO, *Shrinkage Algorithms for MMSE Covariance Estimation*, IEEE Transactions on Signal Processing, 58 (2010), pp. 5016–5029, <https://doi.org/10.1109/TSP.2010.2053029>.
  - [7] N. CHUSTAGULPROM, S. REICH, AND M. REINHARDT, *A hybrid ensemble transform particle filter for nonlinear and spatially extended dynamical systems*, SIAM/ASA Journal on Uncertainty Quantification, 4 (2016), pp. 592–608, <https://doi.org/10.1137/15M1040967>, <https://doi.org/10.1137/15M1040967>, <https://arxiv.org/abs/https://doi.org/10.1137/15M1040967>.
  - [8] COMPUTATIONAL SCIENCE LABORATORY, *ODE test problems*, 2021, <https://github.com/ComputationalScienceLaboratory/ODE-Test-Problems> (accessed 2021-08-27).
  - [9] J. DORMAND AND P. PRINCE, *A family of embedded Runge-Kutta formulae*, Journal of Computational and Applied Mathematics, 6 (1980), pp. 19–26, [https://doi.org/https://doi.org/10.1016/0771-050X\(80\)90013-3](https://doi.org/https://doi.org/10.1016/0771-050X(80)90013-3), <https://www.sciencedirect.com/science/article/pii/0771050X80900133>.
  - [10] G. EVENSEN, *Sequential data assimilation with a nonlinear quasi-geostrophic model using monte carlo methods to forecast error statistics*, Journal of Geophysical Research: Oceans, 99 (1994), pp. 10143–10162, <https://doi.org/https://doi.org/10.1029/94JC00572>, <https://agupubs.onlinelibrary.wiley.com/doi/abs/10.1029/94JC00572>, <https://arxiv.org/abs/https://agupubs.onlinelibrary.wiley.com/doi/pdf/10.1029/94JC00572>.
  - [11] G. EVENSEN, *The Ensemble Kalman Filter: theoretical formulation and practical implementation*, Ocean Dynamics, 53 (2003), pp. 343–367, <https://doi.org/10.1007/s10236-003-0036-9>, <https://doi.org/10.1007/s10236-003-0036-9>.
  - [12] G. EVENSEN AND P. J. VAN LEEUWEN, *An ensemble kalman smoother for nonlinear dynamics*, Monthly Weather Review, 128 (2000), pp. 1852 – 1867, [https://doi.org/10.1175/1520-0493\(2000\)128\(1852:AEKSFN\)2.0.CO;2](https://doi.org/10.1175/1520-0493(2000)128(1852:AEKSFN)2.0.CO;2), [https://journals.ametsoc.org/view/journals/mwre/128/6/1520-0493\\_2000\\_128\\_1852\\_aeksf\\_2.0.co\\_2.xml](https://journals.ametsoc.org/view/journals/mwre/128/6/1520-0493_2000_128_1852_aeksf_2.0.co_2.xml).
  - [13] G. GASPARI AND S. E. COHN, *Construction of correlation functions in two and three dimensions*, Quarterly Journal of the Royal Meteorological Society, 125 (1999), pp. 723–757, <https://doi.org/https://doi.org/10.1002/qj.49712555417>, <https://rmets.onlinelibrary.wiley.com/doi/abs/10.1002/qj.49712555417>, <https://arxiv.org/abs/https://rmets.onlinelibrary.wiley.com/doi/pdf/10.1002/qj.49712555417>.
  - [14] T. M. HAMILL, *Interpretation of rank histograms for verifying ensemble forecasts*, Monthly Weather Review, 129 (2001), pp. 550 – 560, [https://doi.org/10.1175/1520-0493\(2001\)129\(0550:IORHFV\)2.0.CO;2](https://doi.org/10.1175/1520-0493(2001)129(0550:IORHFV)2.0.CO;2), [https://journals.ametsoc.org/view/journals/mwre/129/3/1520-0493\\_2001\\_129\\_0550\\_iorhfv\\_2.0.co\\_2.xml](https://journals.ametsoc.org/view/journals/mwre/129/3/1520-0493_2001_129_0550_iorhfv_2.0.co_2.xml).
  - [15] T. HASTIE, R. TIBSHIRANI, AND J. FRIEDMAN, *The Elements of Statistical Learning: Data Mining, Inference, and Prediction*, Springer series in statistics, Springer, 2001, <https://books.google.com/books?id=VRzITwgNV2UC>.
  - [16] C.-C. HU AND P. J. VAN LEEUWEN, *A particle flow filter for high-dimensional system applications*, Quarterly Journal of the Royal Meteorological Society, 147 (2021), pp. 2352–2374, <https://doi.org/https://doi.org/10.1002/qj.4028>, <https://rmets.onlinelibrary.wiley.com/doi/abs/10.1002/qj.4028>, <https://arxiv.org/abs/https://rmets.onlinelibrary.wiley.com/doi/pdf/10.1002/qj.4028>.
  - [17] B. R. HUNT, E. J. KOSTELICH, AND I. SZUNYOGH, *Efficient data assimilation for spatiotemporal chaos: A local ensemble transform kalman filter*, Physica D: Nonlinear Phenomena, 230 (2007), pp. 112–126.
  - [18] R. JORDAN, D. KINDERLEHRER, AND F. OTTO, *The variational formulation of the fokker-planck equation*, SIAM Journal on Mathematical Analysis, 29 (1998), pp. 1–17, <https://doi.org/10.1137/S0036141096303359>, <https://doi.org/10.1137/S0036141096303359>, <https://arxiv.org/abs/https://doi.org/10.1137/S0036141096303359>.
  - [19] D. P. KINGMA AND J. BA, *Adam: A method for stochastic optimization*, arXiv preprint arXiv:1412.6980, (2014).
  - [20] P. KLOEDEN AND E. PLATEN, *Numerical Solution of Stochastic Differential Equations*, Stochas-

- tic Modelling and Applied Probability, Springer Berlin Heidelberg, 2011, <https://books.google.com/books?id=BCvtssom1CMC>.
- [21] A. KOLMOGOROFF, *Über die analytischen methoden in der wahrscheinlichkeitsrechnung*, Mathematische Annalen, 104 (1931), pp. 415–458.
- [22] S. KULLBACK AND R. A. LEIBLER, *On information and sufficiency*, The annals of mathematical statistics, 22 (1951), pp. 79–86.
- [23] Q. LIU AND D. WANG, *Stein variational gradient descent: A general purpose Bayesian inference algorithm*, in NIPS, 2016.
- [24] E. LORENZ, *Predictability: a problem partly solved*, in Seminar on Predictability, 4-8 September 1995, vol. 1, Shinfield Park, Reading, 1995, ECMWF, ECMWF, pp. 1–18, <https://www.ecmwf.int/node/10829>.
- [25] E. N. LORENZ, *Deterministic nonperiodic flow*, Journal of Atmospheric Sciences, 20 (1963), pp. 130 – 141, [https://doi.org/10.1175/1520-0469\(1963\)020<0130:DNF>2.0.CO;2](https://doi.org/10.1175/1520-0469(1963)020<0130:DNF>2.0.CO;2), [https://journals.ametsoc.org/view/journals/atsc/20/2/1520-0469\\_1963\\_020\\_0130\\_dnf\\_2\\_0.co\\_2.xml](https://journals.ametsoc.org/view/journals/atsc/20/2/1520-0469_1963_020_0130_dnf_2_0.co_2.xml).
- [26] A. A. POPOV AND A. SANDU, *A bayesian approach to multivariate adaptive localization in ensemble-based data assimilation with time-dependent extensions*, Nonlinear Processes in Geophysics, 26 (2019), pp. 109–122.
- [27] A. A. POPOV AND A. SANDU, *An explicit probabilistic derivation of inflation in a scalar ensemble kalman filter for finite step, finite ensemble convergence*, 2020, <https://arxiv.org/abs/2003.13162>.
- [28] A. A. POPOV, A. N. SUBRAHMANYA, AND A. SANDU, *A stochastic covariance shrinkage approach to particle rejuvenation in the ensemble transform particle filter*, Nonlinear Processes in Geophysics Discussions, (2021), pp. 1–14.
- [29] M. PULIDO AND P. J. VAN LEEUWEN, *Sequential Monte Carlo with kernel embedded mappings: The mapping particle filter*, Journal of Computational Physics, 396 (2019), pp. 400–415, <https://doi.org/https://doi.org/10.1016/j.jcp.2019.06.060>, <https://www.sciencedirect.com/science/article/pii/S0021999119304681>.
- [30] V. RAO, A. SANDU, M. NG, AND E. D. NINO-RUIZ, *Robust data assimilation using L1 and huber norms*, SIAM Journal on Scientific Computing, 39 (2017), pp. B548–B570.
- [31] S. REICH AND C. COTTER, *Probabilistic forecasting and Bayesian data assimilation*, Cambridge University Press, 2015.
- [32] S. REICH AND S. WEISSMANN, *Fokker–Planck Particle Systems for Bayesian Inference: Computational Approaches*, SIAM/ASA Journal on Uncertainty Quantification, 9 (2021), pp. 446–482, <https://doi.org/10.1137/19M1303162>, <https://doi.org/10.1137/19M1303162>, <https://arxiv.org/abs/https://doi.org/10.1137/19M1303162>.
- [33] S. ROBERTS, A. A. POPOV, A. SARSHAR, AND A. SANDU, *Ode test problems: a matlab suite of initial value problems*, arXiv preprint arXiv:1901.04098, (2021).
- [34] S. R. SAHANI PATHIRAJA, *Discrete gradients for computational Bayesian inference*, Journal of Computational Dynamics, 6 (2019), pp. 385–400.
- [35] O. SAN AND T. ILIESCU, *A stabilized proper orthogonal decomposition reduced-order model for large scale quasigeostrophic ocean circulation*, Advances in Computational Mathematics, 41 (2015), pp. 1289–1319, <https://doi.org/10.1007/s10444-015-9417-0>, <https://doi.org/10.1007%2Fs10444-015-9417-0>.
- [36] T. STEIHAUG AND A. WOLFBRANDT, *An attempt to avoid exact jacobian and nonlinear equations in the numerical solution of stiff differential equations*, Mathematics of Computation, 33 (1979), pp. 521–534, <http://www.jstor.org/stable/2006293>.
- [37] P. TANDEO, P. AILLIOT, J. RUIZ, A. HANNART, B. CHAPRON, A. CUZOL, V. MONBET, R. EASTON, AND R. FABLET, *Combining analog method and ensemble data assimilation: Application to the lorenz-63 chaotic system*, in Machine Learning and Data Mining Approaches to Climate Science, V. Lakshmanan, E. Gilleland, A. McGovern, and M. Tingley, eds., Cham, 2015, Springer International Publishing, pp. 3–12.
- [38] P. TRANQUILLI, S. R. GLANDON, A. SARSHAR, AND A. SANDU, *Analytical Jacobian-vector products for the matrix-free time integration of partial differential equations*, Journal of Computational and Applied Mathematics, 310 (2017), pp. 213–223, <https://doi.org/https://doi.org/10.1016/j.cam.2016.05.002>, <https://www.sciencedirect.com/science/article/pii/S0377042716302199>, Numerical Algorithms for Scientific and Engineering Applications.
- [39] D. L. VAN KEKEM, *Dynamics of the lorenz-96 model: Bifurcations, symmetries and waves*, (2018).
- [40] P. J. VAN LEEUWEN, H. R. KÜNSCH, L. NERGER, R. POTTHAST, AND S. REICH, *Particle filters for high-dimensional geoscience applications: A review*, Quarterly Journal of the Royal Meteorological Society, 145 (2019), pp. 2335–2365, <https://doi.org/https://doi.org/>

- 10.1002/qj.3551, <https://rmets.onlinelibrary.wiley.com/doi/abs/10.1002/qj.3551>, <https://arxiv.org/abs/https://rmets.onlinelibrary.wiley.com/doi/pdf/10.1002/qj.3551>.
- [41] R. VERSHYNIN, *High-dimensional probability: An introduction with applications in data science*, vol. 47, Cambridge university press, 2018.